8

Preparation and Characterization of Immunosensors for Disease Diagnosis

Antonio Aparecido Pupim Ferreira, Cecílio Sadao Fugivara, Hideko Yamanaka and Assis Vicente Benedetti
Instituto de Química, UNESP - Univ Estadual Paulista
Brazil

1. Introduction

The antigens are viruses, bacteria or part of, toxin or any molecules (organic or inorganic) that is antigenic (may induce an immunological response and can be recognized by antibody). The antibody is a glycoprotein which is produced in response of antigenic attack.
Reaction between antigen and antibody by structural complementation is the base of immunoassay. If the immunological receptor is immobilized on a transducer for detecting a target analyte the device is called immunosensor. Either antibody or antigen could be immobilized on the transducer which converts the biological signal into electrical signal. The immunosensor is classified as optical, mass-sensitive or electrochemical according to the technique. The electrochemical immunosensor, according to the transducer, is classified as amperometric, potenciometric, impedimetric, condutometric.
The cells or organs release trace levels of specific glicoprotein, enzymes and hormones into health patients' serum but the concentrations increase when they are injured. It means that the methodology for clinical diagnosis must be sensitive and with high reproducibility and repeatability. The interaction between antibody and antigen is usually selective presenting high affinity constant (around 10^{15}). Therefore immunosensors are being applied for diagnosis of various diseases states and also to improve effective drug administration.
Studies on immunosensors like potenciometric (Tang et al., 2005), condutometric (Lu et al., 2009), piezeletric (Ren et al., 2008, Sener et al., 2010, Pohanka et al., 2007), fiber optic (Kwon et al., 2002), scanning tunnelling microscopy (Lee et al., 2009) have been published for disease diagnosis. State of immunoassay technologies for tumor diagnosis (Wu et al., 2007) and environmental analysis have been reviewed recently (Farre´ et al., 2009).
The results obtained by immunosensor must have reproducibility and repeatability in order to diagnose the disease or to monitor the disease treatment. Such properties are reached when the system is well optimized and characterized. On this chapter the amperometric and impedimetric devices will be focused on the preparation and characterization of the immunosensor in order to improve its performance.
Usually the complex formed by the affinity reaction between the antigen-antibody is not electrochemically active. It is possible to monitor the reaction by amperometric technique by using an enzyme as tracer like classical ELISA (enzyme-linked immunesorbed assay); in this case instead of absorbance the current intensity is measured. The immunosensor where the affinity reaction is monitored by tracer is indirect and the format could be classified as

sandwich, competitive or indirect (Tijssen, 1985). On the other hand, the impedimetric immunosensor is based on impedance measurement of the electrical equivalent circuit of the oscillator. Consequently no label is necessary to monitor the affinity reaction.

The kind of electrochemical transducer and technique of receptor immobilization play an important role on the selectivity of the immunosensor. For instance, gold screen printed electrode was used for *Trypanosoma cruzi* (*T. cruzi*) protein immobilization through self assembled monolayer (SAM) in order to diagnose Chagas disease (Ferreira et al., 2005). Anti-human cardiac myoglobin antibody immobilized on carbon screen printed electrode by passive adsorption (O'Regan, et. al, 2002) was applied as biochemical marker for acute myocardial infarction (myoglobin) detection; carbon screen printed electrode modified by multiwall carbon nanotubes (MWCNT) and gold nanoparticles was the platform to immobilize the antibody *P. falciparum* for malaria diagnose (Sharma et al., 2008). Glassy carbon electrode (GCE) was modified by Nafion® for competitive detection of anti-schistosoma japonicum antibody (Zhou et al., 2003); modified with multiwall carbon nanotubes integrated with microfluidic systems for quantification of prostate specific antigen in human serum samples (Panini et al., 2008); Fe_3O_4 magnetic nanoparticles/chitosan composite film modified GCE for ferritin determination (Wang & Tan, 2007); GCE functionalized Au nanoparticles for cancer cells detection (Wang & Tan, 2007); bi-layer nano-Au and nickel hexacyanoferrates nanoparticles modified GCE for determination of carcinoembryonic antigen (Yuan et al., 2009). Phenylboronic acid conjugated thiol-mixed monolayer on gold wire (Wang et al., 2008) was proposed for alfa fetoprotein (AFP) detection; such antigen was also detected by microfluidic cell (Maeng et al., 2008); gold nanowire to differentiate between lung and colon cancer (Patil et al., 2008). Graphite–epoxy composite (GEC) electrodes as a platform to immobilize tissue transglutaminase were employed for the autoimmune disorder celiac disease (Pividori et al., 2009), silver epoxy–graphite composite for cardiac troponins detection (Silva et al., 2010).

Cellular products over-expressed by malignant cells have been used as tumor markers but one marker could not be specific to a particular tumor. In this case an array of immunosensor could be the solution (Wu et al., 2007).

Electrochemical impedance spectroscopy (EIS) has been used as a technique for characterization of electrode surface modification but the analysis of interfacial property changes is useful also to monitor the biorecognition events involving antibody-antigen interaction for disease diagnosis. Silver electrodes for interleukin-12 correlated to the diagnosis of multiple sclerosis (La Belle et al., 2007); electropolymerized nanocomposite film containing polypyrrole, polypyrrolepropylic acid and Au nanoparticles was developed for Interleukin 5 which is associated with several allergic diseases (Chen et al., 2008). Gold and platinum electrodes were investigated to diagonose Chagas disease (Diniz et al., 2003) as well as gold screen printed electrodes (Ferreira et al., 2010). The transglutaminase was immobilized on gold screen printed electrode through polyelectrolyte to diagnose celiac disease (Balkenhohl &Lisdat 2007); the impedance signal after the interaction between the Ag and Ab was amplified by using secondary HRP-labelled antibody; the main advantage of impedimetric methodologies (direct immunosensor) was not applied.

Most of amperometric and impedimetric immunosensors published on the literature have no detailed electrode surface characterization which is important for the reproducibility and stability of the device.

2. Preparation and handling of electrodes

Conventional gold and graphite electrodes, screen-printed electrodes (SPE), electrodes prepared from CD-Rs (CDtrodes), gold and magnetic nanoparticles, carbon-on-metal, carbon nanotubes, carbon paste and others substrates have been used as support matrices (transducers) to immobilize biological compounds. The manner of preparation and handling of electrodes are very important for the stability and packing of self-assembled monolayers (SAM) or films and subsequent modifications steps of the analytical methodology.

On cleaning screen-printed electrodes for sensors some recommendations, before the first modification step, were previously described in the literature: washing the SPE gold-based electrode with ethanol or acetone (Ferreira et al., 2010; Navrátilová & Skaládal, 2004; Kaláb & Skládal, 1995), or surface pretreatments for the immunosensors development (Escamilla-Gomez et al., 2009). Carpini et al. gave the following information about pretreatment of SPE gold-based electrodes: "*Although mechanical or electrochemical cleaning of the gold surface is usually recommended, both thiol-tethered DNA probe immobilization and naphthol electrochemistry are not significantly affected by surface pretreatments. Thus, screen-printed gold electrodes were used as produced*" (Carpini et al., 2004); Xu et al. also used as received SPE gold-based electrode for HRP immobilization (Xu et al., 2003).

Recently, García-González et al. characterized different SPE-gold electrodes used for sensors preparation and the electrodes were used without pretreatment (García-González et al., 2008). Escamilla-Gomez et al. used gold screen-printed electrodes (AuSPEs) pretreated with acid solution (H_2SO_4) for impedimetric immunobiosensors. AuSPES were obtained from different manufacturers, then various cyclic voltammograms were recorded and the electrodes washed with deionized water (Escamilla-Gomez et al., 2009). The SPE gold-based electrode, depending on the manufacturing, is not exactly a gold electrode, so the acid treatment used for cleaning their surfaces cannot be applied. Sometimes modifications may occur mainly on the surface of the reference electrode and for this reason aggressive medium cannot be used for cleaning this type of SPE electrodes (Ferreira et al., 2010).

It is important to know that the SPE used in the immunosensors construction must be in an aluminum sealed package in which each electrode is individually isolated from the atmosphere, or in special boxes also protected from the atmosphere. In the case of the locked package of one electrode, it should only be opened just before use and the surface must be protected against any contamination. Obviously, if this care is not taken in consideration the SPE electrodes are improper to use for sensors preparation and even for electrochemical studies. SPE electrodes stored in aluminum sealed package or in other way can sometimes undergo oxidation and then they must be rejected. Another important factor to be considered on the SPE use for one specific study is the utilization of electrodes which belong to the same manufacturing batches. Differences between batches are linear. It means that different batches result in different output signal by scale not by shape. If the response is calibrated by internal standard, such calibration will be valid for all batches (production in series). Using different batches absolute reproducibility of the immunosensors cannot be ensured.

When conventional gold surface is used, the pretreatment procedures can be mechanical, chemical and electrochemical (Campuzano et al., 2002, 2006; Hoogvliet et al., 2000). The influence of the different surface pretreatments on the immunosensor response of a polycrystalline gold electrode should be studied (Carvalhal et al., 2005). Gold transducers

are very often used because of the facility to obtain a stable assembled layer. Thiol and disulphide groups quickly adsorb on gold surfaces, and over longer periods covalent bonds are formed (Godínez, 1999). Cysteamine ($HS-CH_2-CH_2-NH_2$), for example, a thiol with a short chain length, has two functional groups that can be used as a bridge between the electrode and other kinds of layers. The stability and organization of monolayer depend on the length of the chains between the terminal and free groups and also on the lateral interactions between chains. Short chains can lead to the formation of a less stable and more disorganized layer (Mendes et al., 2008). SBZA (4-(methylmercapto)-benzaldehyde) can also be used to produce self-assembled monolayers to prepare gold surfaces for further modification and presents the advantage that it substitutes, for instance, cysteamine and glutaraldehyde since both S-H and CHO groups are present in this molecule. However, special care is needed with its incubation due to its high solubility in ethanol, and also the monolayer must be formed under refrigeration and humid atmosphere (Conoci et al., 2002).
Many other kinds of molecules may form self-assembled monolayers to immobilize biological molecules or materials in order to develop immunosensors: fullerene-C_{60}, ferrocene, ionic liquid (1-siobutyl-3-methylimidazolium bis(trifluoromethylsulfonyl)amine) (Xiulan et al., 2011), electropolymerized thionine (Tang et al., 2008), lysine (Wang et al., 2010), hydroquinone (Xuan et al., 2003), aminosilane (Parker et al., 2009).
Biological molecules or materials can be immobilized on the SAMs or modified SAMs or, in some cases directly on the electrode surface. In the latest case, special attention should be given to the loss of activity due to some steric impediment involving electroactive sites.
The influences of the immobilization processes on the immunossensor performance were evaluated with different transducers, antigens and antibodies. Considering the various steps involved in the immunosensor construction, very important details must be considered in the analytical procedure of antigen incubation. The results obtained for shorter antigen incubation times may be a consequence of some partial leaching of antigen due to an unstable self-assembled monolayer formation, while those for longer incubation times may indicate a possible degradation of the modified electrode surface, with loss of layer integrity. Therefore, a detailed study to optimize the incubation time of antigen in the development of biosensors is strongly recommended (Ferreira et al., 2010).
The immobilization of antibodies on solid-phase materials has been used for the development of the immunosensor and different procedures were described in the literature. Problems associated with biological activity of the antibodies on immobilization have been observed in many cases (Lu et al., 1996). The interactions antigen-antibody are complexes by nature and the reproducible response characteristic of immunosensors requires that the affinity reaction is minimally disturbed by the fabrication procedure. The random orientation of the asymmetric macromolecules on transducers is one of the main reasons for such loss. Protein A, produced by *Staphylococcus aureus*, is a highly stable receptor capable of binding to the Fc fragment of immunoglobulins and the Fab binding sites of IgG antibody are thus oriented for immuassays reactions (Sjoquist et al., 1972; Lee et al., 2004). Therefore, these binding characteristics of the protein A can be used as an affinity surface in immunosensors construction (Campanella et al., 1999).
Magnetic nanoparticles as substrate for biomolecules immobilization are a special alternative used in recent years for the construction of immunosensors (Wang & Tan, 2007; Tang et al., 2008). Due to their attractive properties, magnetic nanoparticles have been used in immunology (Ao et al., 2006), cell separation processes or purging processes (Bittencourt

et al., 2006; Sonti & Bose, 1995). Several applications of magnetic nanoparticles in the immobilization of immunoglobulines have also been reported (Pham & Sim, 2010; Smith et al., 2006).
Other conditions affecting the immunosensor response characteristics must be critically examined: they include the purity of the reagents, incubation temperature in different steps of immunoassay, ionic strength and solution composition, working pH range, condition of the electrode surface and the oxygen content of the solution.

3. Techniques for surface control and immunosensor characterization

The preparation and control of the substrate surface and its modification constitute critical steps of the immunosensor development since they must permit the immobilization of biological molecule or material on the electrode surface and the interaction between the modified surface and the sample. The optimization of the incubation time is very critical on the different steps of the immunosensor development.
A detailed characterization of the various steps involved in the immunosensor development can be useful for understanding the contribution of each step on the behavior of the global system, and for further improvement of the analytical process. So, it is strongly recommended that each step of the immunosensor construction be carefully evaluated using different electrochemical and non-electrochemical techniques.
The interpretation of the results obtained by applying, in an adequate manner, appropriate experimental techniques can provide information on the distribution of structural defects, redox properties and the kinetics and mechanism of the monolayer formation or other modifications introduced on the surface, such as ions incorporation, water uptake and so on. The different electrochemical techniques can help understanding the electron transfer and mass transfer processes after each different step of immunosensor building. The non-electrochemical ones may inform on the morphology and topography of the bare and modified surface, on the interaction between the modifier and the surface, on the chemical nature of the bonds and molecules attached on the surface and on the interaction of energy (special by light) with the different entities constituting the system which is being studied, allowing their identification and the knowledge and applications of their properties.

3.1 Electrochemical techniques

Electrochemical techniques are largely used by researchers of different scientific fields due to the fact that the equipment used is of low cost, simple, and easy to utilize and have the advantage of being *in situ* techniques, which allows monitoring the studied system in real time. Many different electrochemical techniques have been used to monitor the response of different surfaces such as gold, graphite, carbon nanotubes, gold nanowires, gold nanoparticles, metallic oxide nanoparticles, spin-on glass surfaces, carbon paste, which can be modified with different modifiers to form SAMs and composites to incorporate active materials and built the desired immunosensor. Each step of this process may be carefully characterized using cyclic voltammetry (CV), electrochemical impedance spectroscopy (EIS), quartz crystal microbalance, chronoamperometry and amperometry, square wave voltammetry (SWV), differential pulse voltammetry (DPV), ellipsometry, and measurements of electrical resistances.

3.1.1 Cyclic voltammetry

For a better understanding of cyclic voltammetry and its general applications the readers can refer to some text books (Noel & Vasu, 1990; Gasser Jr., 1993; Compton & Banks, 2009). As indicated above, cyclic voltammetry (CV) is the electrochemical technique most frequently used to get the first information on the nature of the electrode surface, such as its purity (Angerstein-Kozlowska et al., 1973), stability (Cabot et al., 1991; Benedetti et al., 1991), reproducibility and repeatability (Horta et al., 2009). Sometimes CV is used for cleaning the electrode surface (Calvo et al., 2004); for activating (Tang et al., 2006); and for reconstructing the electrode surface, or to determine the electrode active surface area for small molecules (hydrogen, methanol, CO, ethanol, etc.), which adsorb on the electrode surface (Biegler et al., 1971; Godoi et al., 2009). Cyclic voltammograms obtained for large molecules can be used to determine the real surface area of an electrode, resulting in an area similar to the geometric one (Noel & Vasu, 1990). Such large molecules can be coordination and other inorganic compounds (ferro/ferricyanide, ferrocene/ferrocinium, etc.) and highly solvated ions which may stay in solution without adsorbing on the electrode surface. CV is very often to help establish the global mechanism of an electrochemical process occurring in solution (Naal et al., 1994) or occurring at a surface as nucleation (Noel & Vasu, 1990).

This technique may also indicate some contamination of the electrolyte used as in the case of a phosphate buffer solution, pH 7.4, containing the redox pair $Fe(CN)_6^{-3}/Fe(CN)_6^{-4}$ which was used to characterize the gold electrodes prepared from CDs (CDtrodes). This was observed in our laboratory. Fig. 1 shows the cyclic voltammograms of this system obtained using the same experimental conditions except that the phosphate buffer solution for recording the cyclic voltammogram of Fig. 1b was changed. It is clearly seen that the cyclic voltammogram in Fig. 1a was distorted probably by some impurity that came from the solution that adsorbed on the electrode surface and partially blocked it. This conclusion was drawn after testing all the other possibilities, such as checking cables and all electrical connections, cleaning the electrochemical cell and its components, recording CVs in other equipment, trying several CDtrodes and changing both ferro/ferricyanide salts. The conclusion was that phosphate salts of the buffer solution had been contaminated.

However, it is possible that the main reasons for the large use of cyclic voltammetry is the simplicity of equipment, facilities to scan a large energy range and also a large potential scan rate (from microvolt to hundreds of megavolts per second) which can be coupled with changes in the temperature of the electrochemical cell to study the kinetic of chemical coupled reactions, and mainly its didactical presentation. But sometimes the results of CV are misinterpreted causing some confusing regarding the irreversibility generated by fast chemical coupled reaction or by slow charge transfer reaction. This confusion can be normally distinguished experimentally by changing the scan rate (ν) and / or the temperature of the system. Another common misinterpretation is related to the effect of ohmic drop on the anodic and cathodic peak potentials separation since the ohmic drop presents similar effect as a quasi-reversible process (Taconni et al., 1973). In this case it is important, after checking the position of the electrodes in the cell and the Luggin capillary position respect to the surface of the working electrode, to increase the solution conductivity in order to diminish the uncompensated solution resistance.

A simple example of uncompensated resistance effect (ohmic drop effect) can be observed in Fig. 2 for 4×10^{-3} mol L^{-1} $Fe(CN)_6^{4-}$ ion in KCl aqueous solution where the concentration of the supporting electrolyte was 0.5 or 0.05 mol L^{-1} at different scan rates. Typical E/I profile

can be seen for the redox couple studied with anodic (E_{ap}) and cathodic (E_{cp}) current peaks well-defined. Also, no current peaks appear in the absence of potassium ferrocyanide. The experimental conditions were the same except for the supporting electrolyte concentration, which varied.

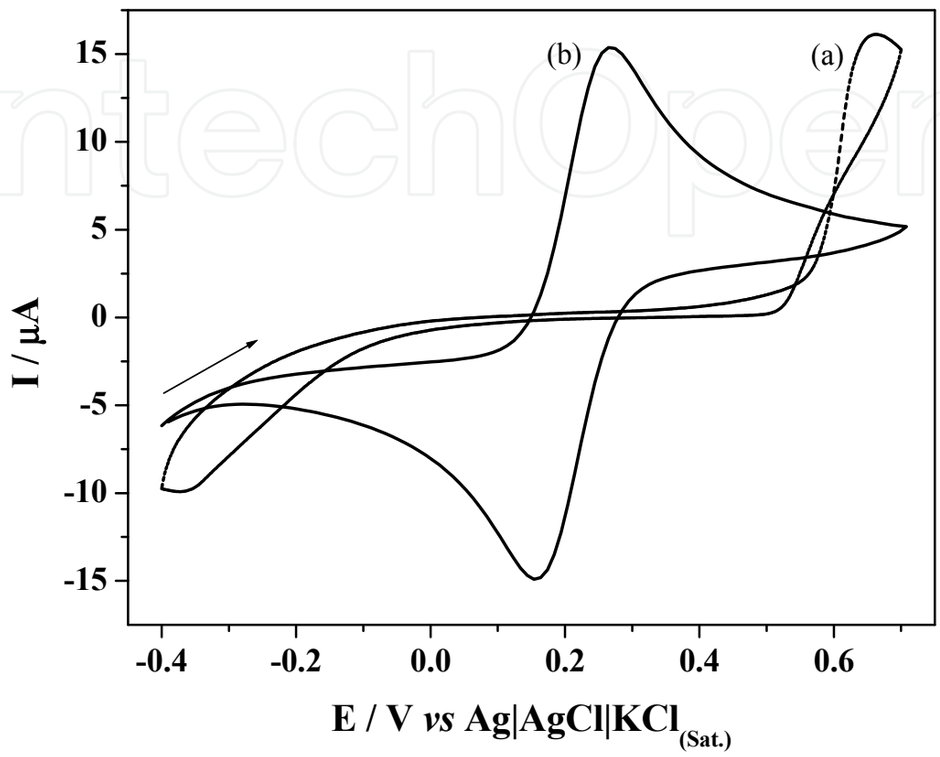

Fig. 1. Cyclic voltamograms of gold CDtrode in 1.0 × 10^{-3} mol L^{-1} $Fe(CN)_6^{3-/4-}$ phosphate buffer solution 0.1 mol L^{-1}, pH 7.4, at 50 mV s^{-1}. The CDtrode was cycled in 2.0 mol L^{-1} H_2SO_4 solution at 50 mV s^{-1}: (a) contaminated phosphate buffer solution; (b) cleaned phosphate buffer solution (Reproduced by permission of M.V. Foguel).

The main differences between these cyclic voltammograms were the separations between the anodic and cathodic peaks (ΔE_p) and the difference between the anodic or cathodic current peaks. For 0.5 mol L^{-1} KCl the values of ΔE_p were around 60 mV in 0.5 mol L^{-1} KCl (Fig. 2a) for all scan rates measured, while in 0.05 mol L^{-1} KCl, ΔE_p varied from 80 to 120 mV for $5 \geq \nu/\text{mV s}^{-1} \geq 100$ (Fig. 2b). CVs recorded in 0.05 mol L^{-1} KCl aqueous solution present all the characteristics of an increase in the uncompensated solution resistance as ν increases: augment in the peak potential separation, decrease in current peaks and rounding of the peaks. The effect of current migration is very low for 0.05 mol L^{-1} KCl and completely negligible for 0.5 mol L^{-1} KCl in aqueous solution (Bard & Faulkner, 1980). In a parallel experiment, CVs were recorded for a solution containing 2.0 × 10^{-2} mol L^{-1} $Fe(CN)_6^{3-}$ + 2.0 × 10^{-2} mol L^{-1} $Fe(CN)_6^{4-}$ in the absence of KCl salt. The peak potentials were separated by more than 150 mV at 50 mV s^{-1} and the peak current was lower than the current measured when KCl was present. It means that the sum of migration and diffusion currents was unable to overcome the influence of the ohmic drop, leading to a lower instead of a higher total current. The decrease in the peak current was caused by the solution resistance.

Feldberg (Feldberg, 2008) simulated the effect of uncompensated resistance on the cyclic voltammetric response of an electrochemically reversible surface-attached redox couple assuming an uniform current and potential distribution across the electrode surface. The similarity of the effect of voltammetric responses for a slow electrochemical reaction and the uncompensated resistance is evident, which may cause misinterpretation of the mechanism of the electrode process. It is also common to attribute the linear current peak, I_p – $v^{1/2}$ relationship to diffusion, but sometimes nucleation or other processes can follow the same relationship (Noel & Vasu, 1990).

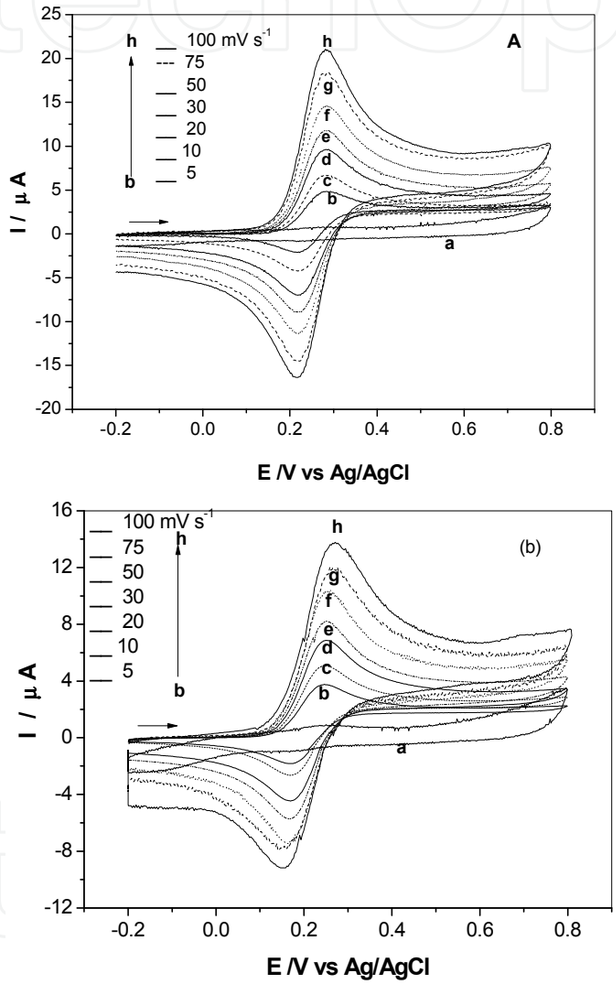

Fig. 2. Cyclic voltammograms for Pt in 4 x 10^{-3} mol L^{-1} $Fe(CN)_6^{4-}$ ion + KCl aqueous solution (**a**) 0.5 and (**b**) 0.05 mol L^{-1}, at 25 ^oC, geometric area of the working electrode of 0.027 cm^2 and at different scan rates.

As seen above, the CV has been often used to characterize immunosensors and many times a phosphate-based buffer solution is used, which may present effect of uncompensated resistance due to its low conductivity, resulting in cyclic voltammograms for $Fe(CN)_6^{3-}$ /$Fe(CN)_6^{4-}$ redox couple away from that expected for a one-electron reversible process under diffusion control. For this reason, phosphate buffer saline solution shows cyclic

voltammograms with a better definition since it shows lower effect of uncompensated solution resistance maintaining all other parameters and conditions constant. For instance, Figure 3 shows two cyclic voltammograms for screen printed electrode and gold electrode in 1.0×10^{-2} mol L^{-1} $Fe(CN)_6^{4-}$, 0.1 mol L^{-1} phosphate buffer solution, pH 6.9, at 50 mV s^{-1} and 25 ^oC. The anodic and cathodic peak potential separation (ΔE_p) values are higher than 59.15 mV/n and therefore the electrode process cannot be described as one-electron charge transfer under diffusion control. It is well known that phosphate buffer solutions pH near 7 and salts concentrations around 0.1 mol L^{-1} present no classical response expected for a completely reversible process. The main reasons for that are the deviation of a reversible process, which leads to a response of a quasi-reversible system, and the influence of ohmic drop. Both of them increase the (ΔE_p) values. It is probable that both effects are present in the CVs of Fig. 3.

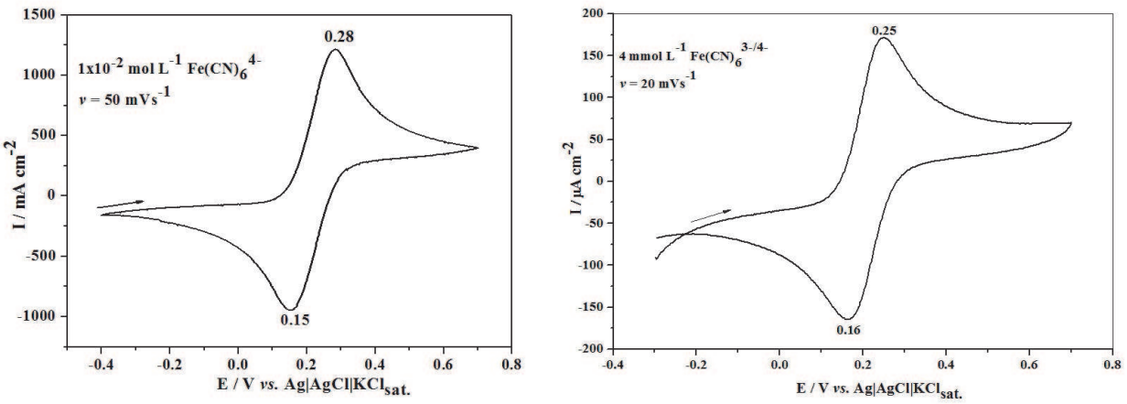

Fig. 3. Cyclic voltammograms for bare (a) gold-CDtrode ($A_{geom.}$ =0.071 cm^2) and (b) gold electrode ($A_{geom.}$ =0.0227 cm^2) in 0.1 mol L^{-1} phosphate buffer solution, pH 6.9, containing potassium forrocynide, at 25^oC.

Cyclic voltammograms for a bare gold electrode recorded in 2.0×10^{-3} mol L^{-1} $Fe(CN)_6^{3-/4-}$, 0.1 mol L^{-1} phosphate buffer solutions, pH ≈ 7, at 25 mV s^{-1} resulted in ΔE_p = 90 mV (Campuzano et al., 2006), while in 2.5×10^{-3} mol L^{-1} $Fe(CN)_6^{3-/4-}$, 0.01 mol L^{-1} phosphate buffer, 0.1 mol L^{-1} KCl, pH 7.0, at 50 mVs^{-1}, a ΔE_p = 65 mV was measured (Pei et al., 2001). It is evident that the phosphate buffer saline (PBS) solution presents higher conductivity and is recommended whenever possible.

When 0.5 mol L^{-1} $NaClO_4$ plus 1×10^{-3} mol L^{-1} $Fe(CN)_6^{4-}$ was used, at 100 mV s^{-1} a ΔE_p = 70 mV was measured (Janeck et al., 1998). The idea that ohmic drop effect is present at lower concentrations of supporting electrolyte can be also inferred from the following results: 0.1 mol L^{-1} $NaClO_4$ and 0.1 mol L^{-1} KCl with 2×10^{-3} mol L^{-1} $Fe(CN)_6^{3-/4-}$, pH 7.0, at 25 mV s^{-1}: ΔE_p = 140 mV and 150 mV, respectively (Campuzano et al. 2006). However, recently Cho et al. (Cho et al., 2008) measured a ΔE_p = 100 mV for 2.5×10^{-3} mol L^{-1} $Fe(CN)_6^{3-/4-}$, 0.5 mol L^{-1} KCl at 50 mV s^{-1}. When CVs were recorded for different screen printed gold electrodes (SPE) in 1×10^{-3} mol L^{-1} $Fe(CN)_6^{3-}$ ion + 0.1 mol L^{-1} H_2SO_4 aqueous solution at 100 mV/ s ΔE_p = 62 to 76 mV and at 2000 mV s^{-1} ΔE_p = 78 to 231 mV were obtained, suggesting some influence of SPEs, mainly at higher potential scan rates (García-González et al., 2008). It is important to note that the conductivity of the sulfuric acid solution is higher than phosphate buffer and 0.1 mol L^{-1} KCl or $NaClO_4$ resulting in a lower ΔE_p value.

When an electrode is modified with self-assembled monolayer, or other modifiers, a barrier may be formed on the electrode surface, which in some extension hinders the charge transfer reaction. So, this effect can be studied by analyzing the changes in the electrochemical response of a reversible or quasi-reversible redox reaction of some electroactive species present in solution. Cyclic voltammetry of electroactive species such as $Fe(NC)_6^{3-/4-}$, ferrocinium/ferrocene, and others which can be used as markers, is a valuable and convenient tool for monitoring the barrier effect of the modified electrode, since the electron transfer between the electrode and species in solution must occur by tunneling either through the barrier or through the defects in the barrier. The tunneling electron transfer is expected to occur when the surface is completely covered by the modifier and an electron transfer via pinholes when it occurs at the defects of the modifier layer, situation where the microelectrode approach could be used. Having in mind a barrier effect, the surface coverage can be estimated from CVs resulting in a semi-quantitative analysis of this effect. So, in general, slight distortions on CVs compared to the bare electrode are expected when the modifiers produce a low surface coverage, which means that the access to the electroactive species from the solution to the electrode occurs without significant impediment. A great distortion on CVs suggests a strong barrier effect, limiting the access of the electrode surface by the markers present in the solution. Based on these ideas the surface coverage could be estimated from cyclic voltammograms assuming linear diffusion to bare areas by the equation (Janeck et al., 1998):

$$\theta_{CV} = 1 - (I_{p,mod}/I_{p,bare}) \quad (1)$$

where $I_{p,mod}$ and $I_{p,bare}$ represent the peak currents for the marker on the modified and bare electrodes, respectively. Different factors influence the cyclic voltammetric response: surface roughness, dominance of radial diffusion near each defect site (Janeck et al., 1998), the presence of positive or negative charge on the modifier can electrostatically interact with the marker increasing or decreasing the interaction strength, i.e., facilitating or making the charge transfer more difficult, or influence the lateral interaction by repulsion between the modifiers species (Calvo et al., 2004; Doblhofer et al., 1992; Ferreira et al., 2009). On a surface coverage, $\theta \leq 0.98$ at intermediates scan rates can give peak current intensity almost the same as the one obtained for a bare electrode, and a $\theta = 0.9945$ may show only 30% of decreasing in the peak current (Sabatani & Rubinstein, 1987).

Attention must be paid in using equation (1) to estimate the surface coverage, and generally, its values are lower than those obtained by other techniques including electrochemical impedance spectroscopy. Amatore et al. (Amatore et al., 1983) demonstrated that equation (1) is inappropriate for describing the fractional coverage of electrode surface due to the dominance of radial diffusion near each pinhole or defect site, and also the charge transfer reaction occurs without significant impediment. For instance, when cysteamine (CYS) and CYS and glutaraldehyde (GA) are used to form SAMs on gold-based electrodes, the surface coverage is low, around 0.10 for CYS-SPE and 0.35 for GA-CYS-SPE, and the charge transfer reaction involving the marker occurs similarly as in the bare electrode, with very low impediment (Ferreira et al., 2009). In this case tunneling of electron through the film can be ruled out (Porter et al., 1987) and probably the electroactive species reached the electrode through the large SAM free space of the electrode surface.

However, in the immunosensor characterization, CV was used to choose the better working potential for amperometric analysis (Stefan & Aboul-Enein, 2002; Zhou et al., 2003) and also

to detect the presence of SAM and other modifiers on the electrode surface. CV was also used to evaluate if the SAM of hydroquinone on the gold electrode acted as a mediator of the redox reaction with pyruvate in phosphate buffer saline (PBS) solution, pH 7.4. Anodic and cathodic peak currents depending on the pyruvate solution concentration were observed after 5 min of dropping pyruvate solution on the pyruvate oxidase-adsorbed nylon membrane placed on the top of a gold electrode. The result allowed to conclude that SAM of hydroquinone acted as a good electron mediator for charge transport between pyruvate oxidase-adsorbed nylon membrane and the gold electrode (Xuan et al., 2003). It is easy to denote the presence of the SAM, for instance, on gold electrode since it can be oxidized to form gold oxides which are reduced to metallic gold again. A fresh gold electrode was evaluated before and after thiol deposition by means of a triangular potential scanning (Tlili et al., 2004) and it was observed that the oxidation reaction was reduced and no cathodic current peak was observed after the SAM formation of thiol. The stability of o-quinone produced on glassy carbon electrode modified with single-walled carbon nanotubes was confirmed by CV (Panini et al., 2008). Calvo et al. (Calvo et al., 2004) synthesized the redox polymer $Os(byp)_2ClPyCH_2NH$ poly(allylamine) (PAH-Os) and deposited on the thiolated (SAM of sodium 3-mercapto-1-propanesulfonate) gold electrode forming a bilayer, which was modified with antibiotin IgG and a supramolecular structure was constructed layer-by-layer. This structure responded catalytically to the presence of hydrogen peroxide when HRP is attached to PAH-Os/IgG multilayer. The cyclic voltammetry was used to confirm the presence of osmium in the PAH-Os/IgG multilayer self-assembled structure on gold and evaluate the electrode process involving the redox Os(III)/Os(II) pair in the presence and absence of hydrogen.

Cyclic voltammetry can also be used to increase the performance of the electrode surface, as in the case of highly oriented antibody on gold nanoparticle surface, which has its activity strongly influenced by the surface properties of the transducer (Lu et al., 1995). In this case, the existence of multiple states of adsorbed proteins involving multipoint hydrophobic, electrostatic, and hydrogen bond was assumed for the different surfaces and protein interactions caused by the unfolding of adsorbed proteins. It means that the surface can be treated in such way in order to change its activity. The influence of a chemical/electrochemical treatment of nanoparticles of gold/thionine-modified carbon paste interface can also be verified using repetitive cyclic voltammetry, which allows observing the evolution of the electrode surfaces along the potential excursion. Repetitive cyclic voltammograms of gold-thionine-carbon paste electrode in acetic/acetate buffer solution, pH 7.0 behaved in a completely different way when recorded before and after electrode treatment with $10\%HNO_3$ + $2.5\%K_2Cr_2O_7$ for 90 s and applying +1.5 V/SCE. The oxidation and reduction peaks decrease or disappear as the number of cycles increases for the electrode without treatment probably due to the removal of the hydrophilic gold nanoparticles and thionine molecules from the electrode. The authors also reported that the solution gradually passed from transparent to opaque. On the contrary, for the treated electrode the cyclic voltammograms improved with the number of cycles, probably because of the thionine molecules could be firmly attached to carbon surface via –Co-NH- structure. It is also possible that some electropolymerization occurs, constructing a third-generation network which could give higher stability to the thionine. The treatment also modified the carbon particles which underwent oxidation to form –COOH groups which can react with $–NH_2$ of thionine to form new –CO-NH- groups. Gold nanoparticles synthesized on

multiwall carbon nanotube screen printed electrodes were also evaluated using cyclic voltammetry before and after modifications having $Fe(CN)_6^{3-/4-}$ as redox probe (Sharma et al., 2008). The MWCNTs were treated with acid solution to produce COOH-MWCNT/SPE and these MWCNTs were mixed in a Nafion® solution. The influence Nafion® concentrations deposited on bare SPE was studied in the presence of the redox probe. The greatest anodic peak current was obtained with 0.1 % Nafion® solution, which was chosen for further experiments. Higher concentrations, mainly 1% of Nafion®, blocked the electrode surface. A series of unmodified and modified SPE with gold nanoparticles (Nano-Au/SPE), MWCNTs (MWCNT/SPE), or gold nanoparticles plus MWCNTs (Nano-Au/MWCNTs/SPE) were studied in 1×10^{-3} mol L^{-1} $Fe(CN)_6^{3-/4-}$, 0.1 mol L^{-1} KCl at 50 mV s^{-1}. All modified electrodes showed a peak current higher than the bare one, which was attributed to the increase of the effective electrode surface area. This result is interesting because the active area increased, but in general, the modification of the electrode leads to a decrease in the anodic or cathodic peak current of the redox probe, except when some catalytic or immunosensor reaction occurs.

Gold nanoparticles and agar-agar solution deposited on graphite SPE generates Nano-gold/SPE and they can be evaluated by cyclic voltammetry performed in a thionine solution as redox probe (Zhao et al., 2007). For instance, in acetate buffer solution the CV behavior of thionine showed that the pair of current peaks decreased and shifted in a negative direction as the pH increased from 4 to 7, indicating that H^+ favored the redox reaction of thionine. To demonstrate the stability of the SPE nine parallel tests were done at pH 5.5 and the anodic potential for thionine was 0.796 ± 0.042 V/Ag|AgCl|KCl (KCl concentration not mentioned), and the peak current was 0.276 ± 0.003 μA, showing good reproducibility. The enzymatic catalysis, which indicates that the system works, was clearly demonstrated when H_2O_2 was added to the thionine solution since the cathodic peak greatly increased and the anodic one disappeared. However, the cathodic current greatly diminished when the immunoreaction (*Vibrio parahaemolyticus*, VP + anti-VP → immunocomplex) was permitted to occur. A similar study was also developed with immunologically-sensitive elements for prostate-specific antigen (PSA) detection using a self-assembled phenylboronic acid monolayer on gold (Liu et al., 2008), and CV together with photometry was applied to detect the formation of imunocomplexes of HRP-conjugated anti-PSA and its antigen.

An interesting application of cyclic voltammetry to characterize immunosensors was recently reported (Parker et al., 2009) for aflotoxin M1 detection using an array of 35 microsquares gold electrodes with 20 μm × 20 μm dimensions and edge-to-edge spacing of 200 μm, which avoids overlapping diffusion layers between neighboring microelectrodes in the array. The marker was 1.0×10^{-3} mol L^{-1} ferrocene monocarboxylic acid in 0.01 mol L^{-1} PBS solution at 5 mV s^{-1}, and a sigmoid response characteristic of steady-state CVs as expected for microelectrodes with a sufficient separation between two adjacent electrodes was obtained. The microelectrode interspacing was made of silicon nitride modified with aminosilane and cross-linked with 1,4-phenylene diisothiocyanate to give a larger modified area and to reduce the effect of surface modification on the electrode surface (microelectrodes). It leads to a signal less attenuated by the immobilized reagents. Afterwards, DNA was incubated and it was thought that only the surface covered with silicon nitride modified by aminosilane and 1,4phenylene diisothiocyanate had been modified with DNA. However, when microsquare platinum electrodes were used the current diminished in comparison to the bare electrode, suggesting that some silane

attached to platinum surface allowing DNA interaction; this reduced the active area for $Fe(CN)_6^{3-/4-}$ reaction. When microsquares of gold were used the current was the same for both bare and DNA-modified electrodes, suggesting that the modification procedure has not significantly covered the gold surface. Certain shielding of $Fe(CN)_6^{3-/4-}$ reaction can be due to the physical coverage of the electrode by DNA and electrostatic repulsion between the negatively charged redox couple ions and the DNA phosphate backbone.
Lately, many other studies were developed using gold nanoparticles attached on a modified glassy carbon electrode, which is normally treated by applying a potential perturbation to produce hydroxyl groups on the surface, and cyclic voltammetry was used to characterize the changes caused by the different surface treatment and modification steps up to the construction of the immunosensor (Yuan et al., 2009; Lai et al., 2009).
In these cases as in many others, in general, cyclic voltammetry was used to identify the presence of modifiers on the surface by analyzing the response of a redox couple on the distortions of the CVs such as separation of peak potentials and blocking of the current. Rarely, cyclic voltammetry was used to estimate the surface coverage, θ, values in immunosensors characterization, which were also compared with those estimated from EIS studies (Ferreira et al., 2009). From CV studies, the values of θ for CYS-SPE, GA-CYS-SPE, Tc85 protein-GA-CYS-SPE were 0.10, 0.35 and 0.84, respectively, while from EIS they were 0.32, 0.34 and 0.99, respectively.

3.1.2 Electrochemical impedance spectroscopy

Electrochemical impedance spectroscopy is a very useful technique to study almost all phenomena occurring at an interface since it can explore a large frequency range covering a vast interval of time constant values. It allows to separate different processes such as capacitive, charge transfer, mass transfer, adsorption/desorption, and so on. For this reason, EIS is a powerful tool for investigating the mechanisms of electrochemical reactions, measuring transport properties of materials, measuring dielectric properties of materials, exploring properties of porous electrodes, investigating passive surfaces, investigating modified electrodes and, more recently, it has often been used to monitor the properties of SAMs, mainly in the presence of a redox couple in the electrolyte solution. It is important to note that the studies in the absence of a redox couple in the working solution are also of great significance to understand the stability, the electrical and physicochemical properties of the modified surface, but are rarely performed in the immunosensors field. The possibilities of using EIS are shown in Fig. 4.
Even considering that EIS is a powerful tool for studying many phenomena, as in the case of other electrochemical techniques, it does not allow the identification of chemical species. For this reason, many non-electrochemical techniques must be used to understand the global process operating on the interface which is being studied.
Where does the power of the EIS technique come from? It is a linear technique and as consequence the results are directly interpreted based on the Linear Systems Theory; if an infinite frequency range is explored, the impedance or admittance contains all of the information that can be obtained from the system by linear electrical perturbation/response techniques; the experimental efficiency is extraordinarily high, it means that a high quantity of information is transferred to the observer compared to the quantity produced by the experiment; the validity of the data is readily determined using integral transform techniques that are independent of the physical processes involved. So, what is the main

problem of using impedance? In general, the major problem resides in the models and mathematics involved in the data interpretation (MacDonald, 2006).
To review the fundamentals and to get more details and applications of impedance electrochemical spectroscopy some text books are recommended (Orazem & Tribollet, 2008; Macdonald, 1987; Gabrielli, 1980).

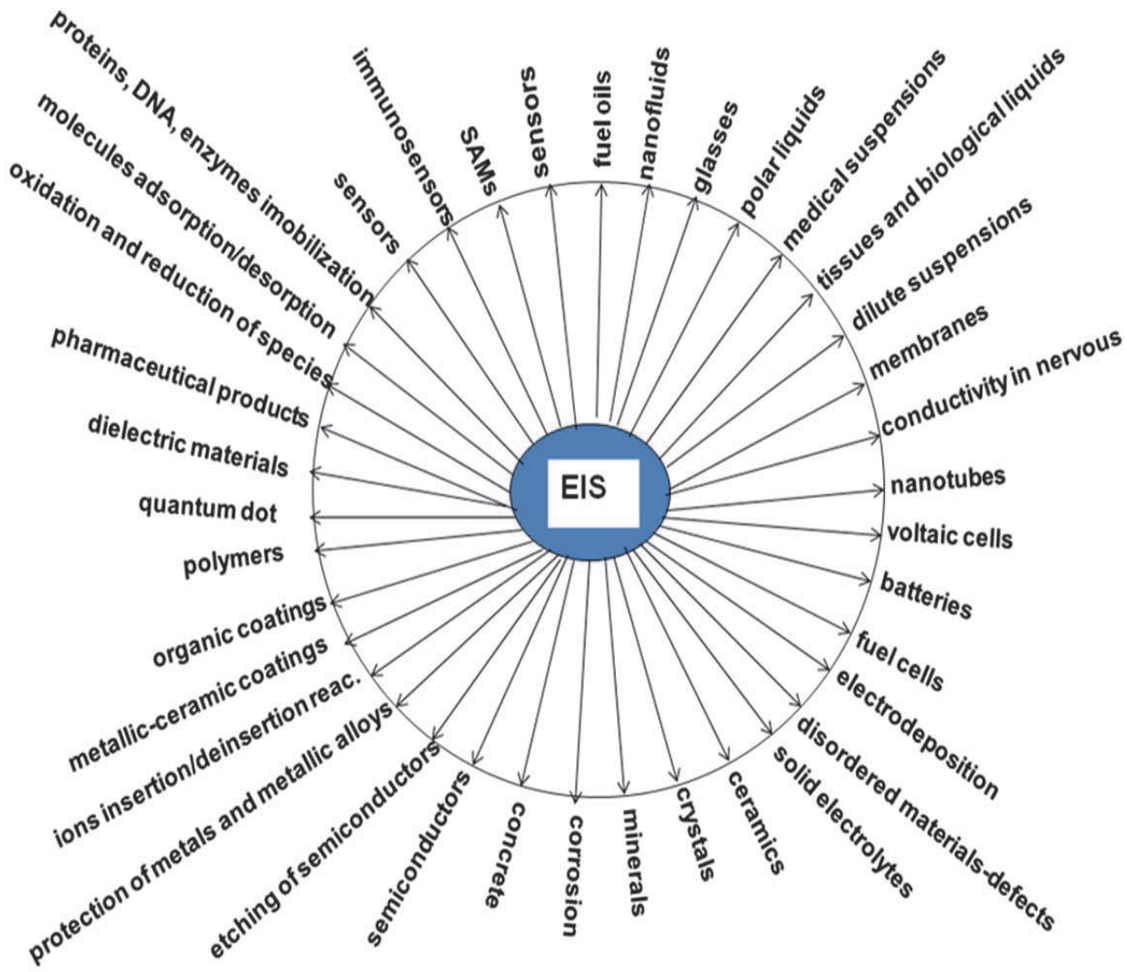

Fig. 4. Some systems that can be studied using EIS.

A great advantage of using EIS is that due to the small amplitude of the sine wave (current or potential) applied to perturb the system respect to its equilibrium or steady state, a sinusoidal perturbation of certain frequency results in a sinusoidal response with the same frequency, although the amplitudes of the entry and exit signals may be different and may present a phase shift. If the perturbation is appropriate the response can be analyzed using the theory of electrical circuits, which can be represented by a proper arrangement of resistors, capacitors and inductors, assuming a linear system. These equivalent electrical circuits (EEC) are models developed to explain the electrochemical impedance data and they must obey at least two conditions (Bonora et al., 1996): all elements of the EEC must have a clear physical meaning and associated to a property of the system which should be able to

produce that electrical response; the EEC must be as simple as possible and generate impedance spectra which are different from the experimental one only by a small defined quantity. The error must be low, not periodical or regular as a function of the frequency.

However, one needs to know that the electrochemical systems are not linear systems, and their response can only approximate of a linear system if, for instance, an enough small perturbation in relation to the equilibrium or steady state is applied to the system. On the other hand, a very small perturbation produces, generally, only a very small response signal, which can be affected by the noise, with a low signal-to-noise ratio. Thus, some requirements must be followed or observed to have a trustful impedance experiment such as linearity, stability and causality (Orazem & Tribollet, 2008, Gabrielli, 1980). It is possible that more than one EEC fits well to the experimental data and the choice by one of them must be based on the knowledge of the physical and physical-chemical phenomena occurring at the interface and on experiments under other conditions.

The obedience to the linearity principle depends on the amplitude of the sine wave, which is governed by the compromise between the desire to minimize the nonlinear response by using small amplitude, and to minimize noise by using a large amplitude perturbation. Therefore, choose the appropriate amplitude value of the sine wave perturbation is always very important to guarantee the best response of the system at each frequency applied and that the system is still exhibiting a linear behavior, which must be experimentally demonstrated. Note that all equipment gave the amplitude of the potential sine wave as rms (root mean square) that is defined as: amplitude $_{rms}$ (mV) = amplitude (mV) × $(\sqrt{2})^{-1}$. To evaluate if the system is or not in a linear regime one can record several impedance diagrams applying different amplitudes keeping all other parameters constant. Afterwards the modulus of impedance (|Z|) values are obtained from the impedance diagrams at certain frequencies (choose one or more frequency values but it is very important to examine the low frequency region since this region is more susceptible to a non-linearly response). The |Z|/|Z| ratio values measured at certain frequency (denominator obtained at 5 mV (rms)) are plotted against the amplitude (rms). Fig. 5 shows the |Z|/|Z| ratio values *vs*. amplitude plot for a carbon paste electrode in 0.1 mol L^{-1} phosphate buffer saline (PBS) solution pH 7.4 containing 1×10^{-3} mol L^{-1} $Fe(CN)_6^{3-/4-}$ ions. This figure clearly indicates that the system responds non-linearly for amplitude (rms) higher than 10 mV at the frequency of 50 mHz.

The stability means that the system should be stable at least during the time course of the experiment. It should be important at the end of an EIS experiment reproduces it beginning the impedance recording from the low to the high frequency, just the opposite that the experiment is normally performed. The causality is another important aspect in electrochemical impedance measurement: it means that no variation in the system can be observed before applying the perturbation. Also, the measured impedance must be finite.

If one compares a simulating with an experimental data set the interpretation of experimental results are rarely simple and further attention is needed. The difficulty may arise from the formation of adsorbed intermediates, which can lead to an adsorption pseudo-capacitance, two separately or partially overlapped semicircles can be shown meaning that the reaction can be more complex than the model; surface heterogeneities are equal to different charge transfer resistances, and also capacitances in a smaller extension; a range of time constants near each other can be a result of differences in the charge transfer kinetic from site to site, producing overlapping of time constants; and surface roughness. All these factors led to a depression of the semicircle causing its center to be below the real impedance axis (Gileadi, 1993; Jorcin et al., 2006) and then a constant phase

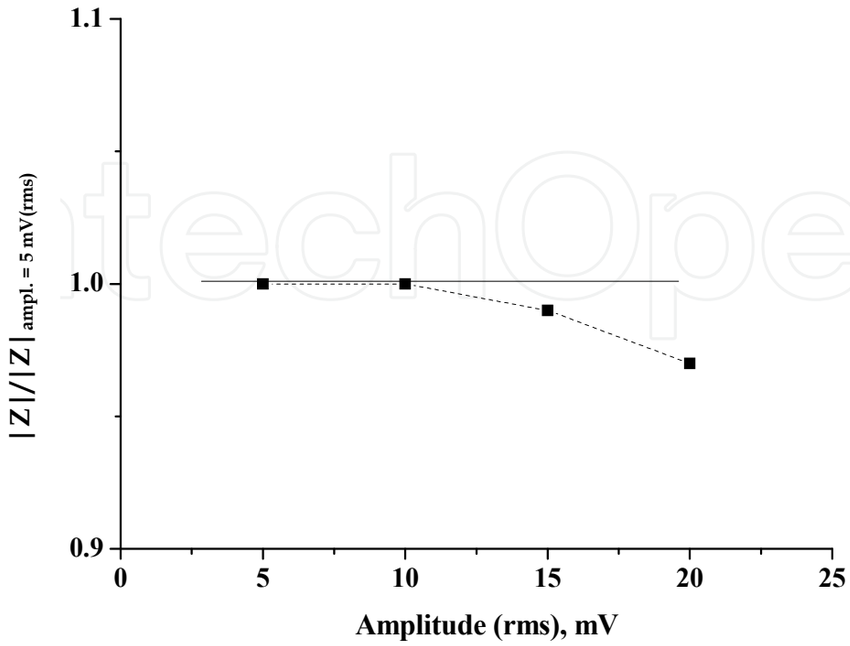

Fig. 5. Modulus of impedance (|Z|) vs. amplitude (rms) for a carbon paste electrode in 0.1 mol L^{-1} phosphate buffer solution pH 7.4 containing 1×10^{-3} mol L^{-1} $Fe(CN)_6^{3-/4-}$ ions at 25°C and 50 mHz.

element (CPE) substitutes a capacitor in EECs (Barsoukov & Macdonald, 2005). For the case that a CPE is parallel with a charge transfer resistance (R_{CT}) to form a "classical" semicircle, the following equation allows to calculate the capacitance value (Hsu & Mansfeld, 2001):

$$C=CPE(\omega_{max})^{n-1}=Y_o(\omega_{max})^{n-1} \quad (2)$$

In this equation Y_o is the canstant phase element parameter, ω_{max} represents the frequency at which the imaginary component reaches a maximum value and n is the exponent. Figure 6 shows the simulation of an EEC with a CPE parallel with a charge transfer resistance with different values of n. The results demonstrated that the depression of the semicircle increases as the n values increase.

Other complications come from the experiment such as non-uniform current distribution caused by the geometry of the cell as a whole or by an excessive approximation of the Luggin capillary of the reference to the working electrode in an effort to minimize the ohmic drop; solution creeping in the crevice formed between the working electrode and its non-conducting holder; changes occurring on the surface during measurement, for instance, corrosion of the working electrode (Gileadi, 1993). It is very important to note that the equations for EIS are based on the assumption that the surface is invariant during the frequency sweeping. It is worse if one scans up to very low frequencies.

All researchers using electrochemical techniques and mainly EIS must be careful and adopt very simple but very important cautions: use shielded cables and cables as short as possible; put the measuring system (electrochemical cell and equipment) in a Faraday cage; connect

the electrical systems to a stabilized voltage; use no-break and excellent ground with wires separated from the electricity cables; do not connect to the stabilized electricity line equipment which can cause noise; avoid working near equipment with significant magnetic field; avoid using a plug located near distribution electricity lines; check switch on and off and other electric switches, electric contacts of electronic plates, cables and alligators clips (sometimes nickel or silver deposition or even metallic welding is recommended); be attentive with other sources of noise like electronic ballast for fluorescent lamp, radio waves, etc.; choose appropriate noise filters; test the potentiostat/galvanostat with a dummy cell (this test does not work for open circuit measurements because of filters only work when the equipment is on, meaning that some potential or current is applied, not at open circuit potential); check if the Luggin capillary is not blocked and so on.

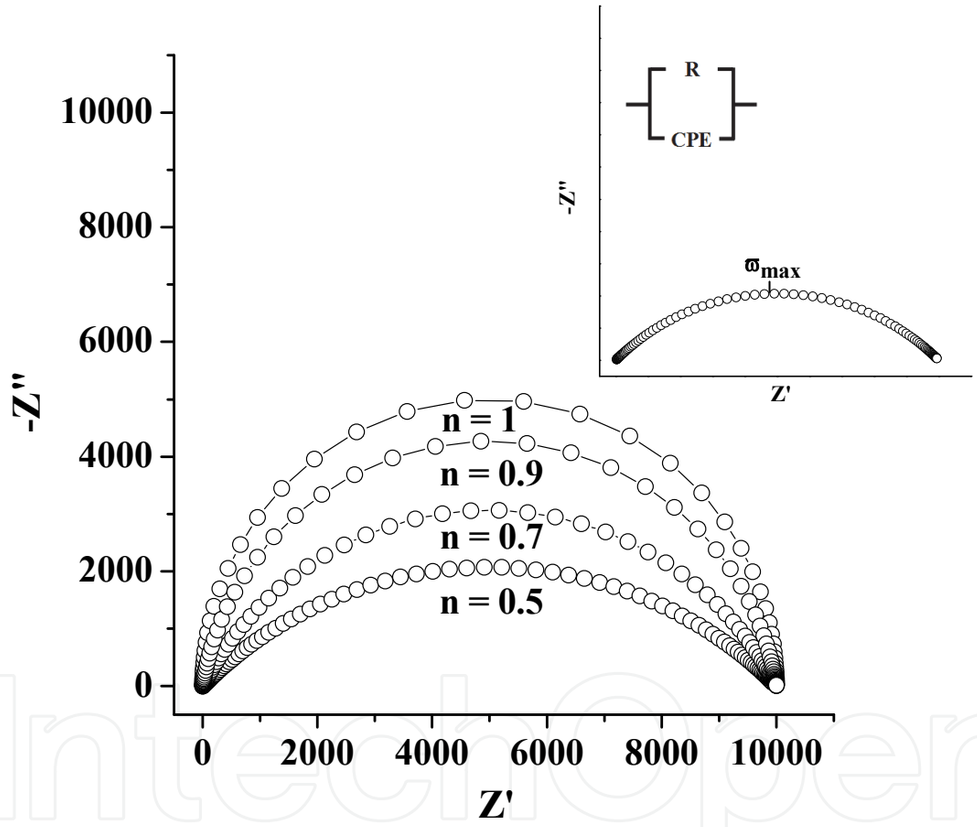

Fig. 6. Simulating impedance diagrams for the ECC showed in the figure for R_{CT} = 10.000 Ω, CPE = 1 × 10^{-5} μF cm^{-2} s^{n-1} and different n values.

An important aspect to be considered in impedance measurement is the working/counter electrodes areas ratio. Considering that both working and auxiliary electrodes are connected in series the capacitance measured of the cell corresponds to the sum of the inverse of both capacitances (C) (Orazem & Tribollet, 2008). The impedance of the cell is given by $Z_{cell} = Z_{WE} + Z_{CE}$ where Z_{WE} is the impedance of the working electrode and Z_{CE} is the counter electrode one. As both electrodes are good electrical conductors the real part of impedance is negligible and the imaginary part is $1/j\omega C$ where ω is the frequency and j is equal √-1.

However, if the area of the counter electrode is 20 times (or more) greater than the working electrode its capacitance is much higher than the capacitance of the working electrode. Therefore, the term $1/j\omega C_{CE}$ is much lower, and the capacitance of the electrochemical cell can be considered as that of the working electrode. Also, the impedance measured is normally not influenced by the one of the reference electrode due to the following facts: a) in terms of resistance or impedance the contribution of the reference is negligible since the entering impedance of the potentiostat is generally equal or greater than 10^{12} Ω, which is much higher than the impedance of the reference; b) in terms of capacitance the contribution of the reference can also be neglected considering the very low current passes through the reference and a Pt wire connected to the reference via a 0.1 μF non electrolytic capacitor can also be used.

These very simple recommendations which seem naïve are mainly for people who are being introduced in electrochemical techniques especially in electrochemical impedance spectroscopy as it is very sensitive to the experimental arrangement.

For each frequency applied only one impedance value is given in the impedance diagram for the system and it is recommended to read 10 to 12 points/decade which should be obtained for a less stable system using a low integration time and for more stable systems a higher integration time. The experimental points of a impedance diagram cannot be connected each other. The integration time means the necessary time to read each point of the impedance diagram with the precision chosen. This time is inserted in EIS acquisition software in different ways depending on the instrument. Therefore, each point in the impedance diagram represents a mean value of a certain numbers of reading and when the instrument cannot read an impedance value at the applied frequency with the precision established by the operator a dispersed point is obtained or the time required is too long to get a point in the impedance diagram. At low frequencies it is more common observe dispersed points due to the long time of measuring.

The impedance measurement represents the response of all components of the system: instrument of measuring, electrochemical cell and connection cables. In this case the limits of the instrument mainly at extreme frequencies or impedance must be considered. The response of an ideal electrochemical cell consisting of resistors and capacitors can be evaluated in an Accuracy Contour plot (Gamry Instruments, 2006) where the following parameters are established: the maximum measurable impedance, the lowest measurable capacitance, the maximum measurable frequency, the low impedance at high frequencies and the lowest measurable impedance. The impedance of an electrochemical cell can also be measured with some accuracy using this type of plot if the data are collected following the EIS theory: linear stationary system without current fluctuation and using an appropriate electrochemical cell.

The maximum impedance that the equipment can measure with accuracy at low frequencies is limited by the current fluctuation in the cell, fluctuation in the current measuring by the instrument and internal resistance. Under this condition the current values measured are very low, for instance, for an impedance of 10^{12} and 10 mV_{rms} the current will be 10^{-14} A, and the noise can significantly influence the measuring, making it important to use of a Faraday cage. This inconvenience can partially be removed by increasing the perturbation amplitude which is limited by the linearity of the system.

The capacitance of the instrument is important for systems like semiconductors, dielectrics and organic coatings (paintings) deposited on metallic substrates. For coatings the

capacitance decreases as its thickness increases, situation in which the capacitance of the instrument can be important.

In general the maximum frequency is limited by the slow response of the components of the potentiostat, its instability, and the slow response of the reference electrode, which can be solved coupling a platinum wire (fast response) to the reference by a non-electrolytic capacitor. The capacitance of this capacitor must be chosen according to the system which is being studied. Systems with low impedance values (batteries and fuel cells) are normally studied at high frequencies where an inductive signal can be obtained. This inductive signal may originate from a physical chemistry process or can be an artifact caused by the inductance of the cell cables.

In the case of low frequencies and low impedances the measurement can be limited by the ability of the potentiostat in allowing the passage of high currents (an amplitude of 10 mV_{rms} with an impedance of 0.01 Ω generates a current of 1 A).

Experimental and simulated data are frequently represented in different formats such as complex plane (Nyquist) plot (Z″ *vs*. Z′ where Z″ is the imaginary and Z′ the real impedance), complex plane admittance plot (-Y″ *vs.* Y′ where Y″ represents the imaginary part of admittance and Y′ the real part), complex plane capacitance plot (C″ *vs.* C′ where C″ represents the imaginary part of capacitance and C′ the real part), Bode impedance modulus *vs*. frequency (log |Z| *vs.* log (f /Hz)) and Bode phase angle *vs*. frequency (-θ or -ϕ *vs.* log (f /Hz)). All complex plane plots must be isometrically represented. Sometimes it is convenient to subtract from the real part of impedance data the solution resistance before plotting the complex plane plots or normalize all complex plane plots to the same values of solution resistance. If the complex plane plots at high frequency show very different values a correction of the Bode phase plot is also recommended. This correction must result in the same values for both real and imaginary values at high frequency (choose a frequency in a stable region).

Regarding immunosensors, the study of the electrochemical impedance response of each step of the electrode modifications, which can be related to the nature of the different surfaces generated, may inform about the charge transport through the layers, surface coverage, and on the influence of antigen or antibody incubation time on the layer stability, mainly distinguishing physical and chemical interactions. EIS can also be used to develop impedimetric sensors.

For the major part of the studies in which the EIS technique was used to characterize each step of an electrode modification $Fe(CN)_6^{3-/4-}$ redox couple was employed as a marker and the data were qualitatively analyzed (Xiulan et al. 2011; Wang & Tan, 2007; Yuan et al., 2009; Wang et al., 2008; Liang et al., 2008). In the Nyquist plot a semicircle at high or middle frequencies followed by a straight line at lower frequencies were frequently observed. The semicircle was attributed to the redox process involving the oxidation and reduction of the marker and the straight line was related to the diffusion-limited process of the species in solution. The amplitude of the semicircle corresponds to the charge transfer resistance (R_{CT}) of the marker oxidation and reduction, the real impedance at highest frequency corresponds to the solution resistance, and the capacitance of the electrical double layer can be obtained from the frequency value at the maximum of the semicircle or from the value of the CPE. The values of the elements of the ECC are obtained by fitting the experimental data with an appropriate EEC which generally corresponds to the Randles circuit where a CPE substitutes the ideal element. The values of R_{CT} generally increased with the modification

steps since the access of marker species to the electrode surface became more difficult and the semicircle overlapped the straight line which may disappear depending on how the electrode surface has been blocked. The values of EEC elements obtained in the simulation must be compared with those previously reported for the same or similar systems (Ferreira et al., 2009).

In some cases the stepwise process of the immunosensor construction was studied by EIS (Yuan et al., 2009)] and the real impedance measured in $Fe(CN)_6^{3-/4-}$ redox couple PBS solution (pH 7.0) was higher for the bare glassy carbon electrode than for the electrode modified with gold nanoparticles due to the increase in the active area of the electrode. In the next step the electrode was modified with nickel hexacianoferrate the charge transfer resistance increased due to the partial blocking of the electrode surface. However, the R_{CT} value decreased again when gold nanoparticles were incorporated to this modified electrode. The decrease of R_{CT} can be related to the increase of the conductivity of the system. When more modifications with organic molecules were performed the R_{CT} increased as expected.

Recently, more detailed studies on the surface modification using EIS with (Ferreira et al., 2009) and without (Ferreira et al., 2010) a redox marker $(Fe(CN)_6^{3-/4-}$ in the solution were performed. In the first study diffusion coefficients of the marker, R_{CT} and C_{dl} values were obtained and compared with data of literature for the bare gold-based SPE. The values of apparent R_{CT} and surface coverage of SPE with CYS, CYS-GA and CYS-GA-Tc85 protein were determined based on a treatment of impedance previously developed for θ values lower (Gueshi et al., 1978; Matsuda et al., 1979) and higher (Finklea et al., 1993) than 0.9. The modified electrode was interpreted as a perforated layer with the transfer reaction occurring at the uncovered regions of the electrode surface which represent defects on the SAM. The changes observed in the cyclic voltammograms and complex plane plots were analyzed considering that the defects are disc-like shapes uniformly distributed over the surface. Therefore the modified electrodes could behave as microarray electrodes with the redox species diffusing to the bottom of the pinholes to undergo charge transfer reaction. For $\theta >$ 0.9 the equations for the impedance were derived for microarray electrodes based on the nonlinear diffusion (Amatore et al., 1983) and from the real faradaic impedance, Z'_f *vs.* $\omega^{-1/2}$ and the appropriate equations R_{CT} and σ (Warburg coefficient) can be obtained when $\omega \rightarrow 0$. The faradaic impedance can be obtained by subtracting the solution resistance from the real part of impedance values (Janeck et al., 1998). The σ value is used to obtain the diffusion coefficient value using equation (3):

$$\sigma = \sqrt{2}\, RT / (n^2F^2CA\sqrt{D}) \quad (3)$$

where R, T and F have their usual meaning, C is the concentration of redox species, A is the geometric area of the electrode, n the number of electrons transferred per molecule or ion, D the diffusion coefficient. From the intersection of the lines at high and low frequency domains the nearest spacing between pinholes can be estimated, and then the values of r_a (mean radii of active area, i.e. pinholes) and r_b (mean radii of inactive area, space between neighbor pinholes). From impedance data the surface coverage were estimated to be around 0.32 for CYS-SPE, 0.34 for GACYS-SPE, and 0.99 for Tc85 protein-GA-CYS-SPE. For $\theta = 0.32$, the radii of individual active regions, and of surrounding inactive regions, were estimated to be 17 and 22 μm, respectively, for both CYS-SPE and GA-CYS-SPE. For the Tc85 protein-GA-CYS-SPE system ($\theta = 0.99$) the estimated radii of pinholes (r_a) and inactive areas (r_b) were 10

and 98 μm, respectively, and the distance between two adjacent pinholes, $2r_b$, was 196 μm. These distances are important to allow and facilitate immunoreactions to occur, and can also be regulated by producing SAMs with molecules of different chain length.

In the second study, electrochemical impedance spectroscopy was used to investigate each step of the procedure employed to modify a screen-printed electrode in pH 6.9 phosphate buffer in the absence of a marker in the solution (Ferreira et al., 2010). The SPE was modified with self-assembled monolayers of CYS followed by GA. Afterwards, the *T. cruzi* antigenic protein Tc85 was immobilized for 2 to 18 hours and bovine serum albumin, BSA, was used to avoid non-specific reactions. The complex plane plots were much more complicated to analyze when compared to the electrodes subjected to the same modification having a redox marker in the working solution. Different EECs have been used to fit the complex plane plots depending on the step of modification. It was demonstrated that phosphate ions adsorb on the electrode surface and the presence of oxygen altered the response of the bare one when compared to the one obtained in its absence. The real impedance values for each step of modification were much higher than those obtained in the presence of the redox marker and increased after each step of surface modification. The modulus of impedance obtained at 10 mHz from the log |Z| vs. log f (not shown) increased in the following order: bare SPE (32 kΩ cm^2) < SPE-CYS (48 kΩ cm^2) < SPE-CYS–GA (53 kΩ cm^2) << SPE-CYS–GA-Tc85 protein (105 kΩ cm^2) << SPE-CYS–GA-Tc85 protein blocked with BSA (575 kΩ cm^2). A very significant result that originated from this investigation using EIS was the influence of the incubation time on the stability of the GA-CYS-SPE incubated with Tc85 protein. The impedance response was extremely dependent of the incubation time. The best incubation time of the Tc85 protein was 6-8 hours.

The total real impedance was very low (around 2 kΩ cm^2) for 2 and 4 h of incubation. A small capacitive semi-circle, followed by an incomplete capacitive arc was observed for 2 h, while an inductive loop was observed for 4 h at low frequencies. The real impedance increased considerably (from around 2 kΩ cm^2 to more than 120 kΩ cm^2) for 6 and 8 h of incubation and for 15 and 18 h incubation the real impedance decreased drastically. For 18 h of incubation an inductive loop was clearly observed, followed by a capacitive arc at lower frequencies. Bode phase plots showed three time constants for curves obtained for 2, 4 and 18 hours of protein incubation while two time constants for curves were recorded after 6, 8 and 15 hours. The interpretation of impedance data was based on physical and chemical adsorption, degradation of the layer at high and middle frequencies and charge transfer reaction involving mainly the reduction of oxygen at low frequencies. In the absence of a redox maker in an aerated phosphate buffer solution, these time constants were interpreted based on physical and chemical adsorption and degradation of the layer at high and middle frequencies, and charge transfer reaction involving mainly the reduction of oxygen at low frequencies (Ferreira et al., 2010). In conclusion, it was demonstrated that the electrochemical impedance spectroscopy is a powerful tool to evaluate the different stages and the integrity of the surface modifications and to optimize the incubation time of protein in the development of immunosensors.

By plotting the differences in R_{CT} values of a redox probe for a modified electrode before and after the assay procedure as a function of the antigen or antibody concentration an impedimetric immunosensor can be developed (Balkenhohl, T. & Lisdat, 2007; Barton et al., 2008; Vig, et al., 2009; Xiulan, et al., 2011). Navrátilová and Skládal (Navrátilová & Skládal, 2004) demonstrated the possibility of monitoring the immunoreaction of

dichlorophenoxyacetic acid herbicide (acid 2,4-D) on SPEs modified with SAMs at a fixed frequency. EIS were also used to study the regeneration of the immunosensor (Liu et al., 2008;Xiulan et al., 2011) by comparing the impedance diagrams and parameters obtained for immnusensors and after removing the antigen or antibody from the surface and following the next steps of immunosensor construction and analysis using the same protocol as before. In general, the first regeneration causes insignificant changes in the immunosensor response, but second and further regenerations diminished the immunosensor efficiency.

3.1.3 Other electrochemical techniques

Quartz crystal microbalance (QCM), ellipsometry, chronoamperometry, amperometry, square wave voltammetry (SWV), diferential pulse voltametry (DPV) and measurements of electrical resistance or conductance have also been used to study the characterization and the assay immunosensors.

The QMC technique has received special attention in the latest years and is based on the application of an antibody coating or an enzyme on a quartz crystal resonator with a cleaning gold surface which will capture a specific pathogen. The capture of the target pathogen increases the mass or viscosity of the environment of the gold surface changing the frequency resonance of the crystal. The impedance of the oscillating quartz crystal exposed to different concentrations of *Salmonella* was measured (Kim et al., 2003). An antibody-coated paramagnetic microspheres captured the *Salmonella* cells and the complex was magnetically moved to the sensing crystal and then captured by immobilized antibodies. The magnetic force was useful to enhance the response of the sensor. Many other studies were developed using the QMC technique to confirm the deposition of biological molecules on self-assembled superstructures and immunosensor assay (Shen et al., 2001; Calvo et al., 2004; Tlili et al., 2004; Mutlu et al., 2008; Boujday et al., 2009). A deep discussion on the use of QMC technique on the step-by-step immunosensor characterization and on immunosensor assay can be found in another specific chapter in this book.

In the immunosensors field the ellipsometry technique is generally used to characterize and understand antibody Langmuir-Blodgett films immobilized on immunoassay surfaces and determine the mean thickness of the films (Tengvall et al., 1998; Preininger et al., 2000; Nagare & Mukherji, 2009).

Chronoamperometry and amperometry techniques were largely used to measure the current and catalytic current generated by applying certain potentials and time during the immunosensors construction and immnunosensors assay (Martins et al., 2003; Ferreira et al., 2005; Zacco et al., 2006; Panini et al., 2008; Pividori et al., 2009).

Square wave voltammetry (SWV) and differential pulse voltammetry (DPV) as analysis techniques are much more sensitive than cyclic voltammetry and amperometry mainly due to the elimination of the background current during the experiment course and for this reason they are frequently used in immunosesors assay (Arias et al., 1996; Wang & Tan, 2007; Tang & Xia, 2008; Yang et al., 2009).

The measurements of electrical resistances or conductance (Tang & Xia, 2008; Maeng et al., 2008) have also been used to characterize immunosensors and in immunosensors assay. In the first case less labor and expensive and shorter time consuming immunosensor than conventional one was developed and in the second case a biosensor system that can be used for simultaneous screening of multiple pathogens in a sample was fabricated and characterized.

3.2 Non-electrochemical techniques

Surfaces modified with SAMs and by the different steps of immunosensors construction have also been characterized using infrared-based techniques including diffuse-reflectance infrared Fourier transform spectroscopy (DRIFTS), Fourier transform infrared spectroscopy (FTIR) and Fourier transform infrared attenuated total reflectance spectroscopy (FTIR-ATR). Infrared-based techniques have successfully been used in many surfaces characterization as adjunct to more well-known spectroscopic methods and are often useful where traditional techniques fail. Transducers modified with SAMs and biological molecules exhibit the conditions required for analysis, otherwise the molecules are diluted with non-absorbing powder such as KBr (Tengvall et al, 1998; Pradier et al., 2002).

Others techniques have been used as X-ray photoelectron spectroscopy (XPS) (Yam et al., 2001), Auger electron spectroscopy (AES) (Yang et al., 2009; Huang & Lee, 2008), contact angle measurements (Martins et al, 2003), surface plasmon resonance (Sigal et al., 1998; Silin et al., 1997), radiolabelling (Tidwell et al., 1997) for immunosensors characterization.

Atomic force microscopy (AFM) has been utilized to analyze the presence of the biological layer on the transducer and to obtain information on the surface morphology of the biological element of the sensor (topography images) or to immobilize the antigen or antibody-coated cantilever as immunosensor transducer, (Takahara et al., 2002; Ferreira et al., 2006; Grogan et al., 2002; Ferreira & Yamanaka, 2006).

The scanning electron microscopy (SEM) and transmission electron microscopy (TEM) were also used (Gan et al., 2010; Lu et al., 2010) since they can inform about the morphology of the unmodified and modified surfaces and on the nature of the nanoparticles used to construct the first step of an immunosensor or added after the end of some specific step to enhance the immunosensor response.

Enzyme-linked immunosorbent assay (ELISA) is a classical method employed in the optimization of the methodology to determine the presence of an immobilized active antibody or antigen and to monitor the lifetime and stability of the immobilized biological molecule and is also used to characterize the steps of immunosensors construction. The spectrophotometric method is used to detect the products of a reaction involving antigen and antibody with enzyme-linked and is essentially important to consider the principle of ELISA methodology on the surface transducer (Grogan et al., 2002; Ferreira et al., 2005).

4. Concluding remarks

The immobilization of antibodies on solid-phase materials has been used for the development of the immunosensor and different procedures were described in the literature. The potentiality of the methodology for disease diagnosis could be transformed into tools for clinical laboratories if the device would be repetitive, reproducible and sensible enough to distinguish the health from the sick person. The stable immobilization of biological compound on the transducer surface and then the surface characterization through electrochemical and non-electrochemical techniques will improve the real application of such devices.

Several electrochemical techniques such as potentiometry, amperometry, differential pulse voltammetry, square wave voltammetry, quartz crystal microbalance and electrochemical impedance have been used to determine the performance of the immunosensors and for analytical applications. However, it was also demonstrated in this chapter that some of these techniques such as cyclic votammetry and mainly electrochemical impedance based on the

microelectrodes theory can be used to have a better idea about the surface coverage and also to estimate the size of pinholes and the mean distance between two adjacent pinholes. This distance is important to allow and facilitate the immunoreactions, and can also be regulate by producing SAMs with molecules of different chain length. It was also suggested that electrochemical impedance can satisfactorily be used to choose the best incubation time of each step of immunosensor construction. EIS may also help to a better understand the changes in the electrochemical response of each step of the immunosensor construction in the absence and presence of a marker since it is a high sensitivity technique and allows separating the contribution of the solution resistance from the other processes occurring at the electrode and solution interface.

The tendency in the immunosensor development seems indicate studies involving microfluidics, immunoarrays, transducers modified with nanoparticles, nanotubes and nanocones to produce devices with high sensitivity and able to be used for simultaneous screening of multiple pathogens.

The challenge is to develop immunosensor with a good performance to allow the point-of-care testing (POCT) it means a clinical results conveniently and immediately to the physician.

5. Acknowledgment

The authors wish to thank FAPESP and CNPq (Proc. 300728/2007-7 and 313307/2009-1).

6. References

Amatore, C.; Saveant, J.M. & Tessler, D.J. (1983). Charge transfer at partially blocked surface. A model for the case of microscopic active and inactive sites. *J. Electroanl. Chem*., 147, 39-51.

Angerstein-Kozlowska, H; Conway, B.E. & Sharp, W.B.A. (1973). The real condition of electrochemically oxidized platinum surfaces. Part I. Resolution of component processes. *J. Electroanal. Chem*., 43, 9-36.

Ao, L.; Gao, F.; Pan, B.; He, R & Cui, D. (2006). Fluoroimmunoassay for antigen based on fluorescence quenching signal of gold nanoparticles. *Anal. Chem*., 78, 1104-1106.

Arias, F.; Godínez, L.A.; Wilson, S.R.; Kaifer, A.E. & Echegoyen, L. (1996). Interfacial hydrogen bonding. Self-assembly of a monolayer of a fullerene-crown ether derivative on gold surfaces derivatized with an ammonium-terminated alkanethiolate. *J. Am. Chem. Soc*., 118, 6086–6087.

Balkenhohl, T. & Lisdat, F. (2007). Screen-printed electrodes as impedimetric immunosensors for the detection of anti-transglutaminase antibodies in human sera. *Anal. Chim. Acta,* 597, 50–57.

Bard, A.J. & Faulkner, L.R. (1980). Electrochemical methods, John Wiley & Sons, N.Y.

Barsoukov, E. & Macdonald, J. R. (2005). Impedance spectroscopy theory, experiment, and applications, John Wiley & Sons, USA.

Barton, A.C.; Davis, F. & Higson, S. P. J. (2008). Labeless immunosensor assay for the stroke marker protein neuron specific enolase based upon an alternating current impedance protocol. *Anal. Chem., 80,* 9411-9416.

Benedetti, A.V.; Nakazato, R.Z.; Sumodjo, P.T.A.; Cabor, P.L.; Centellas, F.A. & Garrido, J.A. (1991). Potentiodynamic behaviour of Cu-Al-Ag alloys in NaOH: A comparative study related to the pure metals electrochemistry. *Electrochim. Acta*, 36, 1409-1421.

Biegler, T.; Rand, D.A.J. & Woods, R. (1971). Limiting oxygen coverage on platinized platinum; relevance to determination of real platinum area by hydrogen adsorption. *J. Electroanal. Chem.*. 29, 269-277.

Bittencourt, R.A.C.; Pereira, H.R.; Felisbino, S.L.; Murador, P.; Oliveira, A.P.E & Deffune, E. (2006). Isolation of bone marrow mesenchymal stem cells. *Acta Ortop. Bras.*, 14, 22-24.

Bonora, P.L.; Defrorian, F. & Fedrizzi, L. (1996). Electrochemical impedance spectroscopy as a tool for investigating underpaint corrosion. *Electrochim. Acta,* 41, 1073-1082.

Boujday, S.; Méthivier, C.; Beccard, B. &Pradier, C.-M. (2009). Innovative surface characterization techniques applied to immunosensor elaboration and test: Comparing the efficiency of Fourier transform–surface plasmon resonance, quartz crystal microbalance with dissipation measurements, and polarization modulation–reflection absorption infrared spectroscopy. *Anal. Biochem.*, 387, 194–201.

Cabot, P.L.; Centellas, F.A.; Garrido, J.A.; Sumodjo, P.T.A.; Benedetti, A.V. & Nakazato, R.Z. (1991). The influence of the electrochemical treatment on copper-aluminum-silver alloys in deaerated 0.5M sodium hydroxide. *J. Appl. Electrochem.,* 21, 446-451.

Calvo, E.J.; Danilowicz, C.; Lagier, C.M.; Manrique, J. & Otero, M. (2004). Characterization of self-assembled redox polymer and antibodies molecules on thiolated gold electrodes. *Biosens. Bioelectron.*, 19, 1219-1228.

Campanella, L.; Attioli, R.; Colapicchioni, C. & Tomassetti, M. (1999). New amperometric and potentiometric immunosensors for anti-human immunoglobulin G determinations. *Sensors Actuators B*, 55, 23-32.

Campuzano, S.; Gálvez, R.; Pedrero, M.; Villena, F.J.M. & Pingarrón, J.M. (2002). Preparation, characterization and application of alkanethiol self-assembled monolayers modified with tetrathiafulvalene and glucose oxidase at a gold disk electrode. *J. Electroanal. Chem.*, 526, 92-100.

Campuzano, S.; Pedrero, M.; Montemayor, C.; Fatás, E. & Pingarrón, J.M. (2006). Characterization of alkanethiol-self-assembled monolayers-modified gold electrodes by electrochemical impedance spectroscopy. *J. Electroanal. Chem.,* 586, 112-121.

Carpini, G.; Lucarelli, F.; Marrazza, G. & Mascini, M. (2004). Oligonucleotide-modified screen-printed gold electrodes for enzyme-amplified sensing of nucleic acids. *Biosens. Bioelectron.*, 20, 167-175.

Carvalhal, R.F.; Freire R.S. & Kubota, L.T. (2005). Polycrystalline gold electrodes: a comparative study of pretreatment procedures used for cleaning and thiol self-assembly monolayer formation. *Electroanalysis,* 17, 1251-1259.

Chen, W.; Lu, Z. & Li, C. M. (2008). Sensitive human interleukin 5 impedimetric sensor based on polypyrrole-pyrrolepropylic acid-gold nanocomposite. *Anal. Chem., 80,* 8485–8492.

Cho, S.H.; Kim, D. & Park, S.-M. (2008). Electrochemistry of conductive polymers 41. Effects of self-assembled monolayers of aminothiophenols on polyaniline films. *Electrochim. Acta,* 53, 3820-3827.

Choa, H.; Parameswaran, M. &Yu, H-Z. (2007). Fabrication of microsensors using unmodified office inkjet printers. *Sensors Actuators B*, 123, 749-756.

Compton, R.G. & Banks, C.E. (2009). Understanding voltammetry, World Scientific. London.

Conoci, S.; Valli, L.; Rella, R.; Compagnini, G. & Cataliotti, R.S. (2002). A SERS study of self-assembled (4-methylmercapto)benzaldehyde thin films. *Mater. Sci. Eng. C*, 22, 183-186.

Diniz, F.B.; Ueta, R.R.; Pedrosa, A.M.C.; Areias, M.C.; Pereira, V.R.A.,; Silva, E.D.; Silva Jr.; J.G., Ferreira A.G.P. & Gomes, Y.M. (2003). Impedimetric evaluation for diagnosis of Chagas' disease: antigen-antibody interactions on metallic eletrodes. *Biosens. Bioelectron.*, 19, 79-84.

Doblhofer, K.; Figura, J. & Fuhrhop, J.-H. (1992). Stability and electrochemical behavior of "self-assembled" adsorbates with terminal ionic groups. *Langmuir,* 8, 1811–1816.

Escamilla-Gomez, V.; Campuzano, S.; Pedrero, M. & Pingarron, J.M. (2009). Gold screen-printed-based impedimetric immunobiosensors for direct and sensitive *Escherichia coli* quantization. *Biosens. Bioelectron.,* 24, 3365-3371.

Farre´, M.; Kantiani, L.; Pérez, S. & Barcelo, D. (2009). Sensors and biosensors in support of EU Directives. *Trends in Anal. Chem.,* 28, 170-185.

Feldberg, S.W. (2008). Effect of uncompensated resistance on the cyclic voltammetric response of an electrochemically reversible surface-attached redox couple: Uniform current and potential across the electrode surface, *J. Electroanal. Chem.*, 624, 45-51.

Ferreira, A.A.P. & Yamanaka, H. (2006). Microscopia de força atômica aplicada em imunoensaios, *Quim. Nova,* 29, 137-142.

Ferreira, A.A.P.; Alves, M.J.M.; Barrozo, S.; Yamanaka, H. & Benedetti, A.V. (2010). Optimization of incubation time of protein Tc85 in the construction of biosensor: Is the EIS a good tool? *J. Electroanal. Chem.*, 643, 1-8.

Ferreira, A.A.P.; Colli, W.; Costa, P.I. & Yamanaka, H. (2005). Immunosensor for the diagnosis of Chagas' disease. *Biosens. Bioelectron.,* 21, 175–181.

Ferreira, A.A.P.; Fugivara, C.S.; Barrozo, S.; Suegama, P.H.; Yamanaka, H. & Benedetti, A.V. (2009). Electrochemical and spectroscopic characterization of screen-printed gold-based electrodes modified with self-assembled monolayers and Tc85 protein. *J. Electroanal. Chem.,* 634, 111–122.

Ferreira, A.A.P.; Colli, W.; Alves, M.J.M.; Oliveira, D.R.; Costa, P.I.; Güell, A.G.; Sanz, F.; Benedetti, A.V. & Yamanaka, H. (2006). Investigation of the interaction between Tc85-11 protein and antibody anti-*T. cruzi* by AFM and amperometric measurements. *Electrochim. Acta*, 51, 5046-5052.

Finklea, H.O.; Snider, D.A.; Fedyk, J.; Sabatani, E.; Gafni, Y. & Rubinstein, I. (1993). Characterization of octadecanethiol-coated gold electrodes as microarray electrodes by cyclic voltammetry and ac impedance spectroscopy. *Langmuir,* 9, 3660–3667.

Gabrielli, C. (1980). Identification of electrochemical processes by frequency response analysis, Solartron instrumentation group monograph, The Solartron Electronic group Ltd., Farnborough, England.

Gamry Instruments (2006). Accuracy contour plots – Technical Note, PA, USA.

Gan, N.; Hou, J.; Hu, F.; Zheng, L.; Ni, M. & Cao, Y. (2010). An amperometric immunosensor based on a polyelectrolyte/gold magnetic nanoparticle supramolecular assembly—modified electrode for the determination of HIV p24 in serum. *Molecules*, 15, 5053-5065.

García-González; R., Fernández-Abedul, M.T.; Pernía, A. & Costa-García, A. (2008). Electrochemical characterization of different screen-printed gold electrodes. *Electrochim. Acta*, 53, 3242-3249.

Gasser Jr., D.K. (1993). Cyclic voltammetry - Simulation and analysis of reaction mechanisms, VCH Publishers. Germany.

Gileadi, E. (1993). Electrode kinetics for chemists, chemical engineers, and materials scientists. VCH Publishers, Inc., N.Y.

Godínez, L.A. (1999). Substratos modificados con monocapas autoensambladas: dispositivos para fabricar sensores y estudiar procesos químicos y fisicoquímicos interfaciales. *J. Mexican Chem. Soc.*, 43, 219-229.

Godoi, D. R. M.; Perez, J. & Mercedes Villullas, H. (2009). effects of alloyed and oxide phases on methanol oxidation of Pt-Ru/C nanocatalysts of the same particle size. *J. Phys. Chem.,* C 113, 8518–8525.

Grogan, C.; Raiteri, R.; O'Connor, T.G.M.; Glynn, J.; Cunningham, V.; Kane, M.; Charlton, M. & Leech, D. (2002). Characterisation of an antibody coated microcantilever as a potential immuno-based biosensor. Biosens. Bioelectron., 17, 201-207.

Gueshi, T.; Tokuda, K. & Matsuda, H. (1978). Voltammetry at partially covered electrodes. Part I. Chronopotentiometry and chronoamperometry at model electrodes. *J. Electroanal. Chem.*, 89, 247–260.

He, F.; Shen, Q.; Jiang, H.; Zhou, J.; Cheng, J.; Guo, D.; Li, Q.; Wang, X.; Fu, D. & Chen, B. (2009).Rapid identification and high sensitive detection of cancer cells on the gold nanoparticle interface by combined contact angle and electrochemical measurements. Talanta, 77, 1009–1014.

Hoogvliet, J.C.; Dijksma, M.; Kamp, B. & van Bennekom, W.P. (2000). Electrochemical pretreatment of polycrystalline gold electrodes to produce a reproducible surface roughness for self-assembly: a study in phosphate buffer pH 7.4. *Anal. Chem.,* 72, 2016-2021.

Horta, D.G.; Bevilaqua, D.; Acciari, H.A.; Garcia Jr., O. & Benedetti, A.V. (2009). Optimization of the use of carbon paste electrodes (CPE) for electrochemcial studies of chalcopyrite. *Quím. Nova*, 32, 1734-1738.

Hsu, C.H. & Mansfeld, F. (2001). Technical note: Concerning the conversion of constant phase element Y_0 into capacitance. *Corrosion*, 57, 747-748.

Huang, I.Y. & Lee, M.C. (2008). Development of a FPW allergy biosensor for human IgE detection by MEMS and cystamine-based SAM technologies. *Sensors Actuator* B, 132, 340-348.

Janeck, R.P.; Fawcett, W.R. & Ulman, A. (1998). Impedance spectroscopy on self-assembled monolayers on Au(111): sodium ferrocyanide charge transfer at modified electrodes. *Langmuir,* 14, 3011-3018.

Jorcin, J.-B;Orazem, M.E.; Pébère, N. & Tribollet, B. (2006). CPE analysis by local electrochemical impedance spectroscopy. *Electrochim. Acta*, 51: 1473-1479.

Kaláb T. & Skládal, P. (1995). A disposable amperometric immunosensor for 2,4-dichlorophenoxyacetic acid. *Anal Chim Acta*, 304, 361-368.

Kim, G.-O.; Garth, A. & Letcher, S.V. (2003). Impedance characterization of a piezoelectric immunosensor part II: Salmonella typhimurium detection using magnetic enhancement. *Biosens. Bioelectron.*, 18, 91-99.

Kwon, H.J.; Balcer, H.I. & Kang, K.A. (2002). Sensing performance of protein C immuno-biosensor for biological samples and sensor minimization. *Comparative Biochemistry and Physiology Part A,* 132, 231–238.

La Belle, J.T.; Bhavsar, K.; Fairchild, A.; Das, A.; Sweeney, J.; Alford T.L.; Wang, J.; Bhavanandan V.P. & Joshi, L. (2007).A cytokine immunosensor for multiple sclerosis detection based upon label-free electrochemical impedance spectroscopy. *Biosens. Bioelectron.,* 23, 428–431.

Lee, J.; Kang, D.; Kim, S.; Yea, C.; Oh, B. & Choi, J. (2009). Electrical detection of b-amyloid(1-40)using scanning tunnelling microscopy. *Ultramicroscopy*, 109, 923–928.

Lee, W.; Lee, D.-B.; Oh, B.-K; Lee, W.H. & Choi, J.-W. (2004). Nanoscale fabrication of protein A on self-assembled monolayer and its application to surface plasmon resonance immunosensor. *Enzyme Microb. Tech.*, 35, 678-682.

Liang, R.; Peng, H. & Qiu, J. (2008). Fabrication, characterization, and application of potentiometric immunosensor based on biocompatible and controllable three-dimensional porous chitosan membranes. *J. Coll. Interf. Sci*., 320, 125-131.

Liu, S.; Zhang X.; Wu, Y.; Tu, Y. & He, L. (2008). Prostate-specific antigen detection by using a reusable amperometric immunosensor based on reversible binding and leasing of HRP-anti-PSA from phenylboronic acid modified electrode *Clin. Chim. Acta,* 395, 51–56.

Liu, Y.; Gore, A.; Chakrabartty, S. & Alocilja E.C. (2008). Characterization of sub-systems of a molecular biowire-based biosensor device. *Microchim. Acta,* 163, 49-56.

Lu, B.; Smyth, M.R. & O´Kennedy, R. (1996). Oriented immobilization of antibodies and its applications in immunoassays and immunosensors. *Analyst*, 121, 29R-32R.

Lu, B.; Xie, J.M.; Lu, C.L.; Wu, C. & Wei, Y. (1995). Luminescence quenching behavior of an oxygen sensor based on a Ru(II) Complex dissolved in polystyrene. *Anal. Chem.,* 67, 83-87.

Lu, M.; Lee, D.; Xue W. & Cui, T. (2009). Flexible and disposable immunosensors based on layer-by-layer self-assembled carbon nanotubes and biomolecules. *Sensors and Actuators A,* 150, 280–285.

Macdonald J.R. Editor (1987). Impedance spectroscopy: emphasizing solid materials and systems. John Wiley & Sons, N. Y.

MacDonald, D.D. (2006). Reflections on the history of electrochemical impedance spectroscopy. *Electrochim. Acta*, 51, 1376-1388.

Maeng, J.-H.; Lee, B.-C.; Ko, Y.-J.; Cho, W.; Ahn, Y.; Cho, N.-G.; Lee, S.-H. & Hwang, S. Y. (2008). A novel microfluidic biosensor based on an electrical detection system for alpha-fetoprotein. *Biosens. Bioelectron*., 23, 1319–1325.

Martins, M.C.L.; Fonseca, C.; Barbosa, M.A. & Ratner, B.D. (2003). Albumin adsorption on alkanethiols self-assembled monolayers on gold electrodes studied by chronopotentiometry. *Biomaterials*, 24, 3697–3706.

Mendes, R.K.; Carvalhal, R.F. & Kubota, L.T. (2008). Effects of different self-assembled monolayers on enzyme immobilization procedures in peroxidase-based biosensor development. *J. Electroanal. Chem.,* 612, 164-172.

Mutlu, S.; Çökeliler, D.; Shard, A.; Goktas, H.; Ozansoy, B. & Mutlu, M. (2008). Preparation and characterization of ethylenediamine and cysteamine plasma polymerized films on piezoelectric quartz crystal surfaces for a biosensor. *Thin Solid Films,* 516, 1249–1255.

Naal, Z.; Tfouni, E. & Benedetti, A.V. (1994). Electrochemical behaviour of (N-R-4-Cyanopyridinium)-pentaamminruthenium(II) derivatives in acidic medium. Hydrolysis of coordinated nitriles. *Polyhedron*, 13, 133-142.

Nagare, G.D. & Mukherji, S. (2009). Characterization of silanization and antibody immobilization on spin-on glass (SOG) surface. *Appl. Surf. Sci.,* 255, 3696–3700.

Navrátilová, I. & Skládal, P. (2004). The immunosensors for measurement of 2,4-dichlorophenoxyacetic acid based on electrochemical impedance spectroscopy. *Bioelectrochem.,* 62, 11–18.

Noel, M. & Vasu K.I. (1990). Cyclic voltammetry and the frontiers of electrochemistry, Cambridge University Press. England.

O'Regan, T.M.; O'Riordan, L.J.; Pravda, M.; O'Sullivan, C.K. & Guilbault, G.G. (2002). Direct detection of myoglobin in whole blood using a disposable amperometric immunosensor. *Anal. Chim. Acta,* 460, 141–150.

Orazem, M.E. & Tribollet, B. (2008). Electrochemical impedance spectroscopy.John Wiley & Sons, Inc., Hoboken, N. J.

Panini, N.V.; Messina, G.A.; Salinas, E.; Fernández, H. & Raba, J. (2008). Integrated microfluidic systems with an immunosensor modified with carbon nanotubes for detection of prostate specific antigen (PSA) in human serum samples. *Biosens. Bioelectron*., 23, 1145–1151.

Parker, C.O.; Lanyon, Y.H.; Manning, M.; Arrigan, D.W.M. & Tothill, I.E. (2009). Electrochemical immunochip sensor for aflatoxin M1 detection. *Anal. Chem*., 81, 5291-5298.

Patil, S.J.; Zajac, A.; Zhukov, T. & Bhansali, S. (2008). Ultrasensitive electrochemical detection of cytokeratin-7, using Au nanowires based biosensor. *Sensors and Actuators B,* 129, 859–865.

Pei, R.; Cheng, Z.; Wang, E. & Yang, X. (2001). Amplification of antigen–antibody interactions based on biotin labeled protein–streptavidin network complex using impedance spectroscopy. *Biosens. Bioelectron*., 16, 355-361.

Pham, T.T-H. & Sim, S. J. (2010). Electrochemical analysis of gold-coated magnetic nanoparticles for detecting immunological interaction. *J. Nanopart. Res.*, 12, 227-235.

Pividori, M.I.; Lermo, A.; Bonanni, A.; Alegret, S. & del Valle, M. (2009).Electrochemical immunosensor for the diagnosis of celiac disease. *Anal. Biochem*. 388, 229–234.

Pohanka M.; Pavlis, O. & Skládal, P. (2007). Diagnosis of tularemia using piezoelectric biosensor technology. *Talanta* 71, 981–985.

Porter, M.D.; Bright, T.B.; Allara, D.L. & Chidsey, C.E.D. (1987). Spontaneously organized molecular assemblies. 4. Structural characterization of n-alkyl thiol monolayers on gold by optical ellipsometry, infrared spectroscopy, and electrochemistry. *J. Am. Chem. Soc*., 109, 3559-3568.

Pradier, C.-M.; Salmain, M.; Zheng, L. & Jaouen, G. (2002). Specific binding of avidin to biotin immobilized on modified gold surfaces Fourier transform infrared reflection absorption spectroscopy analysis. *Surf. Sci.,* 502–503, 193–202.

Preininger, C.; Clausen-Schaumann, H.; Ahluwalia, A. & Rossi, D. (2000). Characterization of IgG Langmuir–Blodgett films immobilized on functionalized polymers. *Talanta*, 52, 921–930.

Ren, J.; He, F.; Yi, S. & Cui, X. (2008). A new MSPQC for rapid growth and detection of *Mycobacterium tuberculosis*. *Biosens. Bioelectron.,* 24, 403–409.

Sabatani, E. & Rubinstein, I. (1987). Organized self-assembling monolayers on electrodes. 2. Monolayer-based ultramicroelectrodes for the study of very rapid electrode kinetics. *J. Phys. Chem.*, 91, 6663–6669.

Sener, G.; Ozgur, E.; Yılmaz, E.; Uzun, L.; Say, R. & Denizli, A. (2010).Quartz crystal microbalance based nanosensor for lysozyme detection with lysozyme imprinted nanoparticles. *Biosens. Bioelectron.*, 26, 815–821.

Sharma, M.K.; Rao, V.K.; Agarwal, G.S.; Rai, G.P.; Gopalan, N.; Prakash, S.; Sharma, S.K. & Vijayaraghavan, R. (2008). Highly sensitive amperometric immunosensor for detection of *Plasmodium falciparum* histidine-rich protein 2 in serum of humans with malaria: comparison with a commercial kit. *J. Clin. Microbiol.*, 46, 3759–3765.

Shen, D.; Huang, M.; Chow, L. & Yang, M. (2001). Kinetic profile of the adsorption and conformational change of lysozime on self-assembled monolayers as revealed by quartz crystal resonator. *Sensor Actuators* B, 77, 664–670.

Sigal, G.B.; Mrksich, M. & Whitesides, G.M. (1998). Effect of surface wettability on the adsorption of proteins and detergents. *J. Am. Chem. Soc.*, 120, 3464–3473.

Silin, V.; Weetall, H. & Vanderah, D. (1997). SPR studies of the nonspecific adsorption kinetics of human IgG and BSA on gold surfaces modified by self-assembled monolayers (SAMs). *J. Colloid Interface Sci*., 185, 94–103.

Silva, B.V.M.; Cavalcanti, I. T.; Mattos, A. B.; Moura, P.; Sotomayor, M.T. & Dutra, R. F. (2010). Disposable immunosensor for human cardiac troponin T based on streptavidin-microsphere modified screen-printed electrode. *Biosens. Bioelectron.*, 26, 1062–1067.

Sjoquist, J.; Meloun, B. & Hjelm, H. (1972). Protein A isolated from Staphylococcus aureus after digestion with lysostaphin. *Eur. J. Biochem.*, 29, 572-578.

Smith, J.E.; Wang, L. & Tan, W. (2006). Bioconjugated silica-coated nanoparticles for bioseparation and bioanalysis. *Trends Anal. Chem.*, 25, 848-855.

Sonti, S.V. & Bose, A. (1995). Cell separation using protein-A-coated magnetic nanoclusters. *J. Colloid Interface Sci.*, 170, 575-585.

Stefan, R.-I. & Aboul-Enein, H.Y. (2002). The construction and characterization of an amperometric immunosensor for the thyroid hormone (+)-3,3′,5,5′-tetraiodo-L-thyronine (L-T4). *J. Immunoassay & Immunochem.*, 23, 429–437.

Taconni, N.R.; Calandra, A.J. & Arvía, A.J. (1973). A contribution to the theory of the potential sweep method: charge transfer reactions with uncompensated cell resistnace. *Electrochim. Acta,* 18, 571-577.

Takahara, A.; Hara, Y.; Kojio, K. & Kajiyama, T. (2002). Plasma protein adsorption behavior onto the surface of phase-separated organosilane monolayers on the basis of scanning force microscopy. *Colloid Surf. B: Biointerfaces,* 23, 141–152.

Tang, D. & Xia, B. (2008). Electrochemical immunosensor and biochemical analysis for carcinoembryonic antigen in clinical diagnosis. *Microchim. Acta*, 163, 41-48.

Tang, D.; Yuan, R. & Chai, Y. (2006). Electrochemical immuno-bioanalysis for carcinoma antigen 125 based on thionine and gold nanoparticles-modified carbon paste interface. *Anal. Chim. Acta,* 564, 158-165.

Tang, D.; Yuan, R. & Chai, Y. (2008). Magneto-controlled bioelectronics for the antigen–antibody interaction based on magnetic-core/gold-shell nanoparticles functionalized biomimetic interface. *Bioprocess Biosyst Eng.*, 31, 55-61.

Tang, D.; Yuan, R.; Chai,Y. & Fu, Y. (2005). Study on electrochemical behavior of a diphtheria immunosensor based on silica/silver/gold nanoparticles and polyvinyl butyral as matrices. *Electrochem. Comm.*, 7, 177–182.

Tengvall, P.; Lundstrom, I. & Liedberg, B. (1998). Protein adsorption studies on model organic surfaces: an ellipsometric and infrared spectroscopic approach. *Biomaterials*, 19, 407–422.

Tidwell, C.D.; Ertel, S.I. & Ratner, B.D. (1997). Endothelial cell growth and protein adsorption on terminally functionalized, self-assembled monolayers of alkanethiolates on gold. *Langmuir*, 13, 3404–3413.

Tijssen, P. (1985). Practice and theory of enzyme immunoassays, Laboratory techniques in biochem. and molecular biology v.15, R.H.Burdon, P.H.van Knippenberg (ed.), Elsevier Science Publishers.

Tlili, A.; Abdelghani, A.; Hleli, S. & Maaref, M.A. (2004). Electrical characterization of a thiol SAM on gold as a first step for the fabrication of immunosensors based on a quartz crystal microbalance. *Sensors*, 4, 105-114.

Tokuda, K.; Gueshi, T. & Matsuda, H. (1979). Voltammetry at partially covered electrodes. Part III.Faradaic impedance measurements at model electrodes. *J. Electroanal. Chem.*, 102, 41–48.

Vig, A.; Muñoz-Berbel, X.; Radoi, A.; Cortina-Puig, M. & Marty, J.-L. (2009). Characterization of the gold-catalyzed deposition of silver on graphite screen-printed electrodes and their application to the development of impedimetric immunosensors. *Talanta,* 80, 942–946.

Wang, J.; Zhang, S. & Zhang, Y. (2010). Fabrication of chronocoulometric DNA sensor based on gold nanoparticles/poly(L-lysine) modified glassy carbon electrode. *Anal. Biochem.*, 396, 304-309.

Wang, S.-F. & Tan, Y.-M. (2007). A novel amperometric immunosensor based on Fe_3O_4 magnetic nanoparticles/chitosan composite film for determination of ferritin. *Anal. Bioanal. Chem.*, 387, 703-708.

Wang, Z.; Tu, Y. & Liu, S. (2008). Electrochemical immunoassay for α-fetoprotein through a phenylboronic acid monolayer on gold. *Talanta,* 77, 815–821.

Wu, J.; Fu, Z.; Yan, F. & Ju, H. (2007).Biomedical and clinical applications of immunoassays and immunosensors for tumor markers. Trends in Anal. Chem., 26, 679-688.

Xiulan, S.; Zaijun, L.; Yan, C.; Zhilei, W.; Yinjun, F.; Guoxiao, R. & Yaru, H. (2011). Electrochemical impedance spectroscopy for analytical determination of paraquat in meconium samples using an immunosensor modified with fullerene, ferrocene and ionic liquid. *Electrochim. Acta*, 56, 1117-1122.

Xu, X.; Liu, S. & Ju, H. (2003). A novel hydrogen peroxide sensor via the direct electrochemistry of horseradish peroxidase immobilized on colloidal gold modified screen-printed electrode. *Sensors*, 3, 350-360.

Xuan, G.S.; Oh, S.W. & Choi, E.Y. (2003). Development of an electrochemical immunosensor for alanine aminotransferase. *Biosens. Bioelectron.,* 19, 365-371.

Yam, C.-M.; Pradier, C.-M.; Salmain, M.; Marcus, P. & Jaouen, G. (2001). Binding of biotin to gold surfaces functionalized by self-assembled monolayers of cystamine and cysteamine: Combined FT-IRRAS and XPS characterization. *J. Coll. Interface Sci.*, 235, 183–189.

Yang, X.; Yuan, R.; Chai, Y.; Zhuo, Y.; Hong, C.; Liu, Z. & Su, H. (2009). Porous redox-active Cu_2O–SiO_2 nanostructured film: Preparation, characterization and application for a label-free amperometric ferritin immunosensor. *Talanta,* 78, 596-601.

Yuan, Y.-R.; Yuan, R.; Chai, Y.-Q.; Zhuo, Y. & Miao, X.-M. (2009). Electrochemical amperometric immunoassay for carcinoembryonic antigen based on bi-layer nano-Au and nickel hexacyanoferrates nanoparticles modified glassy carbon electrode. *J. Electroanal. Chem.,* 626, 6–13.

Zacco, E.; Pividori, M.I. & Alegret, S. (2006). Electrochemical biosensing based on universal affinity biocomposite platforms. *Biosens. Bioelectron.*, 21, 1291–1301.

Zhao, G.; Xing, F. & Deng, S. (2007). A disposable amperometric enzyme immunosensor for rapid detection of Vibrio parahaemolyticus in food based on agarose/nano-Au membrane and screen-printed electrode. *Electrochem. Comm*., 9, 1263-1268.

Zhou, Y.-M.; Wu, Z.-Y.; Shen, Z.-L & Yu, R.-Q. (2003). An amperometric immunosensor based on Nafion-modified electrode for the determination of *Schistosoma japonicum* antibody. *Sensors & Actuators* B, 89, 292-298.

Biosensors for Health, Environment and Biosecurity

Edited by Prof. Pier Andrea Serra

ISBN 978-953-307-443-6
Hard cover, 540 pages
Publisher InTech
Published online 19, July, 2011
Published in print edition July, 2011

A biosensor is a detecting device that combines a transducer with a biologically sensitive and selective component. Biosensors can measure compounds present in the environment, chemical processes, food and human body at low cost if compared with traditional analytical techniques. This book covers a wide range of aspects and issues related to biosensor technology, bringing together researchers from 16 different countries. The book consists of 24 chapters written by 76 authors and divided in three sections: Biosensors Technology and Materials, Biosensors for Health and Biosensors for Environment and Biosecurity.

How to reference

In order to correctly reference this scholarly work, feel free to copy and paste the following:

Antonio Aparecido Pupim Ferreira, Cecilio Sadao Fugivara, Hideko Yamanaka and Assis Vicente Benedetti (2011). Preparation and Characterization of Imunosensors for Disease Diagnosis, Biosensors for Health, Environment and Biosecurity, Prof. Pier Andrea Serra (Ed.), ISBN: 978-953-307-443-6, InTech, Available from: http://www.intechopen.com/books/biosensors-for-health-environment-and-biosecurity/preparation-and-characterization-of-imunosensors-for-disease-diagnosis

INTECH
open science | open minds

InTech Europe
University Campus STeP Ri
Slavka Krautzeka 83/A
51000 Rijeka, Croatia
Phone: +385 (51) 770 447
Fax: +385 (51) 686 166
www.intechopen.com

InTech China
Unit 405, Office Block, Hotel Equatorial Shanghai
No.65, Yan An Road (West), Shanghai, 200040, China
中国上海市延安西路65号上海国际贵都大饭店办公楼405单元
Phone: +86-21-62489820
Fax: +86-21-62489821

IntechOpen